Redox-Inactive Metals Modulate the Reduction Potential in Heterometallic Manganese-Oxido Clusters

Emily Y. Tsui, Rosalie Tran, Junko Yano, Theodor Agapie*

Division of Chemistry and Chemical Engineering, Arnold and Mabel Beckman Laboratories of Chemical Synthesis, California Institute of Technology, Pasadena, California 91125
e-mail: agapie@caltech.edu

Supporting Information

Contents

General Considerations

Unless indicated otherwise, reactions performed under inert atmosphere were carried out in oven-dried glassware in a glovebox under a nitrogen atmosphere. Anhydrous tetrahydrofuran (THF) was purchased from Aldrich in 18 L Pure-Pac^{TM} containers. Anhydrous dichloromethane, diethyl ether, and THF were purified by sparging with nitrogen for 15 minutes and then passing under nitrogen pressure through a column of activated A2 alumina (Zapp's). Anhydrous 1,2-dimethoxyethane (DME) was dried over sodium/benzophenone ketyl and vacuum-transferred onto molecular sieves. CD_2Cl_2 was purchased from Cambridge Isotope Laboratories, dried over calcium hydride, then degassed by three freeze-pump-thaw cycles and vacuum-transferred prior to use. ^{1}H NMR spectra were recorded on a Varian 300 MHz instrument, with shifts reported relative to the residual solvent peak. ^{19}F NMR spectra were recorded on a Varian 300 MHz instrument, with shifts reported relative to the internal lock signal. Elemental analyses were performed by Midwest Microlab, LLC, Indianapolis, IN. UV−Vis spectra were taken on a Varian Cary 50 spectrophotometer at 25 °C using quartz crystal cells. Electrospray ionization mass spectrometry (ESI-MS) was performed in the positive ion mode using a LCQ ion trap mass spectrometer (Thermo) at the California Institute of Technology Mass Spectrometry Facility.

Unless indicated otherwise, all commercial chemicals were used as received. $Ca(OTf)_2$, NaOTf, $Y(OTf)_3$, and $Zn(OTf)_2$ were purchased from Aldrich. Dimethylferrocene was purchased from Aldrich and sublimed before use. Decamethylferrocene was purchased from Strem. Iodosobenzene,[1] $Sr(OTf)_2$,[2] and dimethylferrocenium triflate[3] were prepared according to literature procedures. $LMn_3(OAc)_3$ and $[LMn_3O(OAc)_3]_2Ca(OTf)_2$ were prepared according to previously published procedures.[4,5] **Caution!** Iodosobenzene is potentially explosive and should be used only in small quantities.

Synthesis of [**1**-Ca(DME)(OTf)][OTf]$_2$

Method A: In the glovebox, a round-bottom flask equipped with a stir bar was charged with $LMn_3(OAc)_3$ (2.0 g, 1.67 mmol) and $Ca(OTf)_2$ (0.90 g, 2.67 mmol, 1.6 equiv). DME (200 mL) was added, and the yellow suspension was stirred at room temperature for 5 min. Iodosobenzene (0.81 g, 3.68 mmol, 2.2 equiv) was added as a solid, and the mixture was stirred at room temperature for 4 h, turning from yellow to purple. The purple solid was collected via filtration, washing with DME, then extracted with dichloromethane. The red-purple solution was concentrated *in vacuo* to yield the product as a red-purple solid (2.45 g, 84%). ^{1}H NMR (CD_2Cl_2, 300 MHz): δ 77.8, 76.5, 72.3, 69.6, 60.5, 53.7, 48.4, 38.6, 37.0, 24.2, 19.9, 17.5, 15.9, 8.1, 3.3, 2.9, −19.3, −23.5, −24.9, −26.4, −29.1 ppm. ^{19}F NMR (CD_2Cl_2): δ −74.4 ppm. UV-Vis (CH_2Cl_2, λ_{max} (ε)): 498 (1410 M^{-1} cm^{-1}), 846 (640 M^{-1} cm^{-1}) nm. Anal. Calcd. For $C_{68}H_{55}CaF_9Mn_3N_6O_{20}S_3$: C, 46.72; H, 3.17; N, 4.81. Found: C, 46.92; H, 3.27; N, 4.89.

Method B: In the glovebox, a scintillation vial equipped with a stir bar was charged with $[LMn_3O(OAc)_3]_2Ca(OTf)_2$ (0.050 g, 0.018 mmol), $Ca(OTf)_2$ (0.011 g, 0.032 mmol, 1.8 equiv) and DME (5 mL). To the stirring suspension, PhIO (0.008 g, 0.036 mmol, 2 equiv) was added as a solid, and the purple mixture was stirred at room temperature, gradually becoming slightly more red after 10 min. After 30 min., the mixture was concentrated *in vacuo* to yield a red-purple solid. The ^{1}H NMR spectrum of a CD_2Cl_2 solution of this unpurified solid matches the ^{1}H NMR spectrum of the product formed in method A.

Synthesis of [**1**-Ca$(OH_2)_3$][OTf]$_3$
Under ambient conditions, [**1**-Ca(DME)(OTf)][OTf]$_2$ (0.046 g, 0.026 mmol) was dissolved in wet acetonitrile and the purple mixture was stirred at room temperature for 5 min. The solvent was removed *in vacuo* to yield a purple solid. This procedure was repeated, and the solid was then dried under vacuum (0.032 g, 71%). ^{1}H NMR (CD_2Cl_2, 300 MHz): δ 77.3, 75.5, 72.0, 59.2, 49.4, 39.1, 36.1, 27.8, 17.4, 16.3, 8.1, −18.2, −23.4, −25.4, −27.1, −28.1 ppm. ^{19}F NMR (CD_2Cl_2): δ −76.8 ppm. Anal. Calcd. for $C_{64}H_{51}CaF_9Mn_3N_6O_{21}S_3$: C, 44.89; H, 3.00; N, 4.91. Found: C, 44.84; H, 3.05; N, 4.73.

Synthesis of [**2**-Ca(DME)(OTf)][OTf]
In the glovebox, a round-bottom flask equipped with a stir bar was charged with [**1**-Ca(DME)(OTf)]$^{2+}$ (0.750 g, 0.429 mmol) and decamethylferrocene (0.140 g, 0.429 mmol, 1 equiv). DME (30 mL) was added, and the purple mixture was stirred at room temperature over 1 h. The gray-purple precipitate was collected on a fritted glass funnel and washed with DME, then extracted with cold THF (40 mL). The purple filtrate was concentrated to ca. 20 mL *in vacuo*, then cooled to −35 °C to precipitate out more Cp*$_2$Fe$^+$, which was filtered off over Celite. The purple filtrate was concentrated *in vacuo* to a purple solid, then recrystallized from DME/CH_2Cl_2/hexanes to yield the product as a purple solid (0.405 g, 59%). ^{1}H NMR (CD_2Cl_2, 300 MHz): δ 65.1, 57.8, 50.7, 41.6, 35.3, 29.6, 15.7, 15.0, 14.2, 8.2, 3.0, −9.6, −12.6, −17.0, −17.9 ppm. ^{19}F NMR (CD_2Cl_2): δ −74.6 ppm. UV-Vis (CH_2Cl_2, λ_{max} (ε)): 495 (710 M^{-1} cm^{-1}), 860 (310 M^{-1} cm^{-1}) nm. Anal. Calcd. for $C_{67}H_{55}CaF_6Mn_3N_6O_{17}S_2$: C, 50.32; H, 3.47; N, 5.26. Found: C, 50.04; H, 3.63; N, 5.06.

Synthesis of [**1**-Sr(DME)(OTf)][OTf]$_2$
In the glovebox, a scintillation vial equipped with a stir bar was charged with L$Mn_3(OAc)_3$ (0.200 g, 0.167 mmol) and Sr(OTf)$_2$ (0.103 g, 0.267 mmol, 1.6 equiv). DME (20 mL) was added, and the mixture was stirred at room temperature for 5 min. PhIO (0.077 g, 0.351 mmol, 2.1 equiv) was added as a solid to the vial, and the mixture was stirred at room temperature for 1 h, turning purple. The purple was precipitate was collected over Celite and washed with DME, then extracted with CH_2Cl_2. The purple CH_2Cl_2 filtrate was concentrated *in vacuo* to yield the product as a purple solid (0.125 g, 42%). ^{1}H NMR (CD_2Cl_2, 300 MHz): δ77.4, 76.2, 72.3, 69.6, 58.9, 51.0, 47.2, 38.8, 36.6, 23.1, 19.3, 17.4, 14.4, 8.2, 3.2, −18.8, −23.1, −26.5, −27.1, −28.1 ppm. ^{19}F NMR (CD_2Cl_2): δ −76.7 ppm. UV-Vis (CH_2Cl_2, λ_{max} (ε)): 497 (1670 M^{-1} cm^{-1}), 845 (725 M^{-1} cm^{-1}) nm. Anal. Calcd. for $C_{68}H_{55}F_9Mn_3N_6O_{20}S_3Sr$: C, 45.48; H, 3.09; N, 4.68. Anal. Calcd. for $C_{69}H_{57}Cl_2F_9Mn_3N_6O_{20}S_3Sr$ ([**1**-Sr(DME)(OTf)][OTf]$_2$•CH_2Cl_2): C, 44.06; H, 3.05; N, 4.47. Found: C, 43.76; H, 3.50; N, 4.46.

Synthesis of [**2**-Sr(DME)(OTf)][OTf]
In the glovebox, a scintillation vial equipped with a stir bar was charged with [**1**-Sr(DME)(OTf)]^2 (0.200 g, 0.111 mmol) and decamethylferrocene (0.036 g, 0.111 mmol, 1 equiv). DME (10 mL) was added, and the mixtre was stirred for 1 h, then cooled to −35 °C for 30 min. Cp*$_2$Fe$^+$ was filtered off over Celite, washing with cold DME. The purple DME filtrate was concentrated *in vacuo*, and the purple solid was recrystallized twice from DME/hexanes to remove the remaining Cp*$_2$Fe$^+$ to yield the product as purple crystals (0.156 g, 85%).
^{1}H NMR (CD_2Cl_2, 300 MHz): δ 62.9, 57.4, 54.4, 35.0, 33.2, 26.1, 22.3, 15.0, 13.3, 9.1, 8.2, 3.4, 3.2, −8.7, −12.4, −15.2, −17.0, −19.9 ppm. ^{19}F NMR (CD_2Cl_2): δ −76.4 ppm. UV-Vis (CH_2Cl_2,

λ_{max} (ε)): 500 (750 M^{-1} cm^{-1}), 850 (330 M^{-1} cm^{-1}) nm. Anal. Calcd. for $C_{67}H_{55}F_6Mn_3N_6O_{17}S_2Sr$: C, 48.87; H, 3.37; N, 5.10. Found: C, 48.60; H, 3.60; N, 5.28.

Synthesis of [**2**-Y(DME)(OTf)][OTf]$_2$
In the glovebox, a scintillation vial equipped with a stir bar was charged with $LMn_3(OAc)_3$ (0.200 g, 0.167 mmol) and $Y(OTf)_3$ (0.134 g, 0.25 mmol, 1.5 equiv). DME (20 mL) was added, and the mixture was stirred at room temperature for 5 min. PhIO (0.077 g, 0.334 mmol, 2.1 equiv) was added as a solid, and the mixture was stirred at room temperature 1 h, turning purple. The purple precipitate was collected over Celite and extracted with CH_2Cl_2. The purple CH_2Cl_2 filtrate was concentrated *in vacuo* and crystallized from CH_2Cl_2/DME/diethyl ether to yield the product as purple crystals (0.055 g, 18%). ^{1}H NMR (CD_2Cl_2, 300 MHz): δ 64.7, 62.6, 59.0, 53.3, 50.9, 41.0, 38.9, 38.2, 36.6, 33.7, 19.6, 16.6, 15.6, 13.6, 13.0, 12.0, 8.0, 3.4, 3.3, −10.8, −15.6, −17.2, −19.3, −20.4, −24.7 ppm. ^{19}F NMR (CD_2Cl_2): δ −77.0 ppm. UV-Vis (CH_2Cl_2, λ_{max} (ε)): 475 (675 M^{-1} cm^{-1}), 806 (260 M^{-1} cm^{-1}) nm. Anal. Calcd. for $C_{68}H_{55}F_9Mn_3N_6O_{20}S_3Y$: C, 45.45; H, 3.08; N, 4.68. Anal. Calcd. for $C_{69}H_{57}Cl_2F_9Mn_3N_6O_{20}S_3Y$ ([**2**-Y(DME)(OTf)][OTf]$_2$•CH_2Cl_2): C, 44.03; H, 3.77; N, 4.47. Found: C, 43.94; H, 3.55; N, 4.40.

Synthesis of [**1**-Na]$_2$[OTf]$_4$
In the glovebox, a scintillation vial equipped with a stir bar was charged with $LMn_3(OAc)_3$ (0.300 g, 0.250 mmol) and NaOTf (0.086 g, 0.501 mmol, 2 equiv). DME (15 mL) was added, and the mixture was stirred for 5 min. PhIO (0.110 g, 0.501 mmol, 2 equiv) was added as a solid, and the mixture was stirred for 1 h, turning purple. The purple heterogeneous mixture was filtered through Celite to remove some purple insolubles, and diethyl ether (ca. 30 mL) was added to the filtrate to precipitate the product as a red-purple solid. This precipitate was collected over Celite, washed with more diethyl ether, then extracted with CH_2Cl_2. The purple extract was concentrated *in vacuo*, then crystallized from CH_2Cl_2/Et_2O to yield the product as a purple crystals (0.072 g, 19%). ^{1}H NMR (CD_2Cl_2, 300 MHz): δ 77.8, 75.6, 71.9, 54.4, 46.7, 45.0, 38.1, 22.5, 17.3, 16.4, 8.5, −16.5, −21.9, −22.5, −25.2, −26.8 ppm. ^{19}F NMR (CD_2Cl_2): δ −78.1 ppm. UV-Vis (CH_2Cl_2, λ_{max} (ε)): 498 (1430 M^{-1} cm^{-1}), 830 (700 M^{-1} cm^{-1}) nm. Anal. Calcd. For $C_{126}H_{90}F_{12}Mn_6N_{12}Na_2O_{30}S_4$: C, 50.72; H, 3.04; N, 5.63. Found: C, 50.40; H, 3.17; N, 5.43.

Synthesis of [**1**-Zn(CH_3CN)][OTf]$_3$
In the glovebox, a scintillation vial equipped with a stir bar was charged with [**1**-Ca(DME)(OTf)]$^{2+}$ (0.255 g, 0.146 mmol) and $Zn(OTf)_2$ (0.068 g, 0.172 mmol, 1 equiv) in CH_3CN (20 mL). The purple solution was stirred at room temperature for 15 min., then concentrated *in vacuo*. The solid was dissolved in CH_2Cl_2, and diethyl ether (10 mL) was added to precipitate out a purple solid, which was collected over Celite and then extracted with CH_2Cl_2. The purple filtrate was crystallized from CH_2Cl_2/diethyl ether to yield the product as a purple solid (0.083 g, 33%). ^{1}H NMR (CD_2Cl_2, 300 MHz): δ 80.1, 75.4, 71.1, 57.3, 52.2, 51.2, 42.1, 40.4, 32.2, 24.3, 21.0, 18.8, 18.1, 15.3, 8.3, 7.5, 6.4, −18.4, −26.1, −28.2, −31.0, −32.0, −36.0 ppm. ^{19}F NMR (CD_2Cl_2): δ −76.4 ppm. UV-Vis (CH_2Cl_2, λ_{max} (ε)): 498 (1430 M^{-1} cm^{-1}), 830 (700 M^{-1} cm^{-1}) nm. Anal. Calcd. For $C_{68}H_{52}Cl_4F_9Mn_3N_7O_{18}S_3Zn$ ([**1**-Zn(CH_3CN)][OTf]$_2$•$2CH_2Cl_2$): C, 43.11; H, 2.77; N, 5.18. Found: C, 42.59; H, 2.66; N, 4.48.

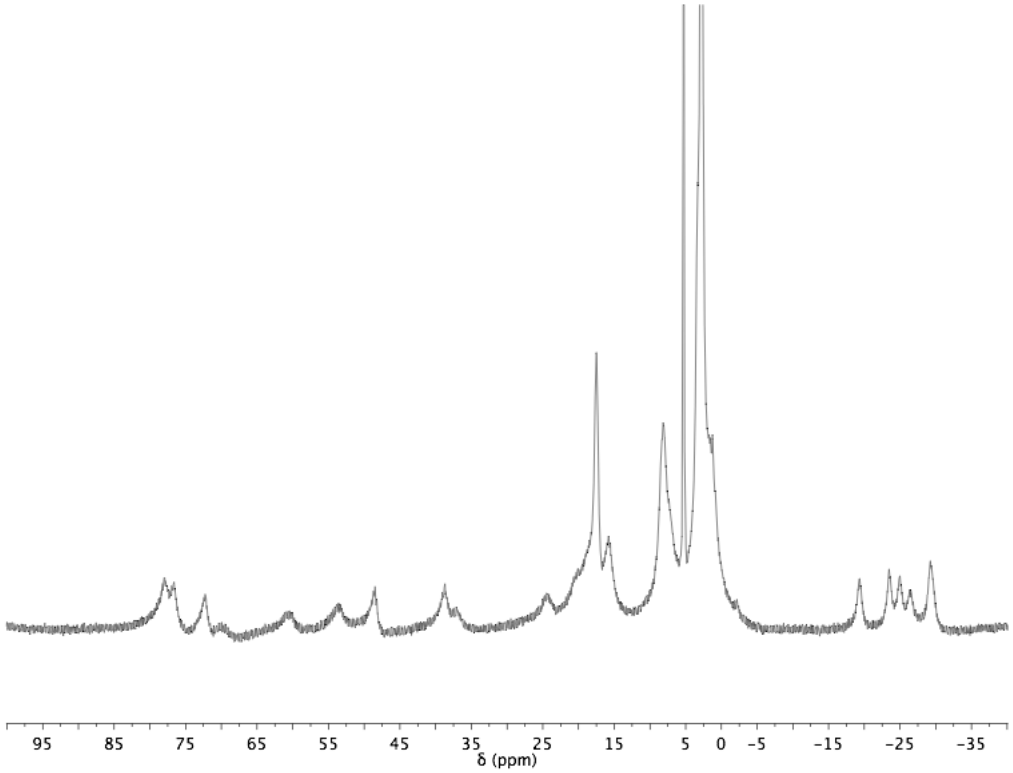

Figure S1. ^{1}H NMR spectrum of [**1**-Ca(DME)(OTf)]$^{2+}$ in CD_2Cl_2 at 25 °C.

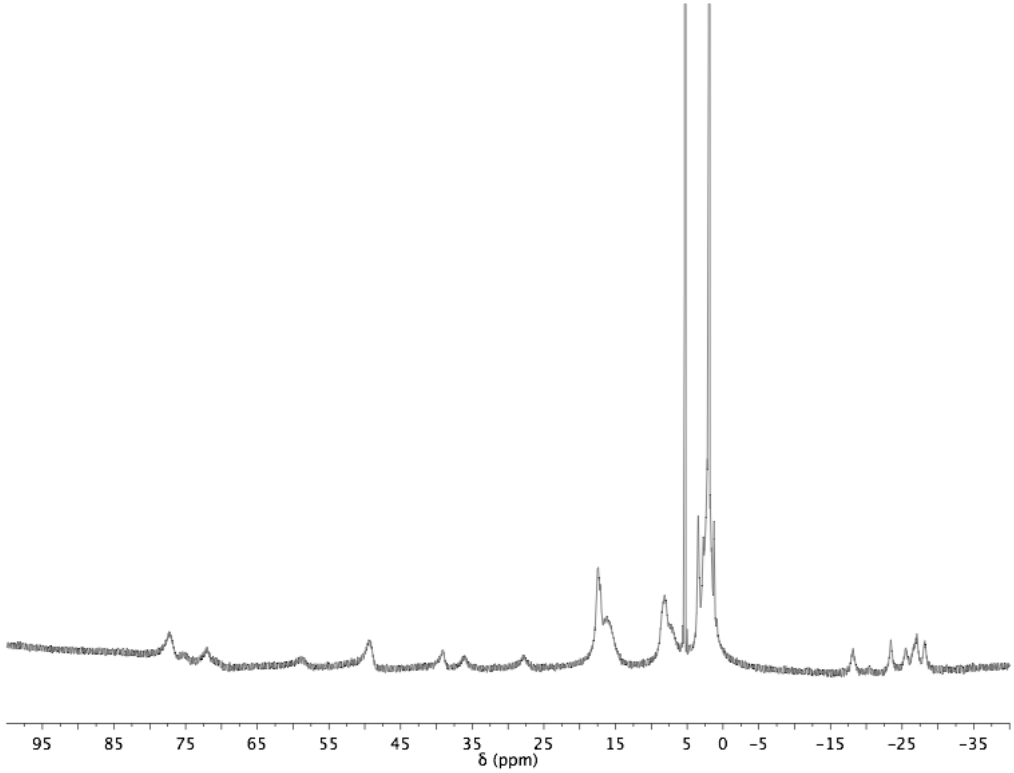

Figure S2. ^{1}H NMR spectrum of [**1**-Ca$(OH_2)_3$]$^{3+}$ in CD_2Cl_2 at 25 °C.

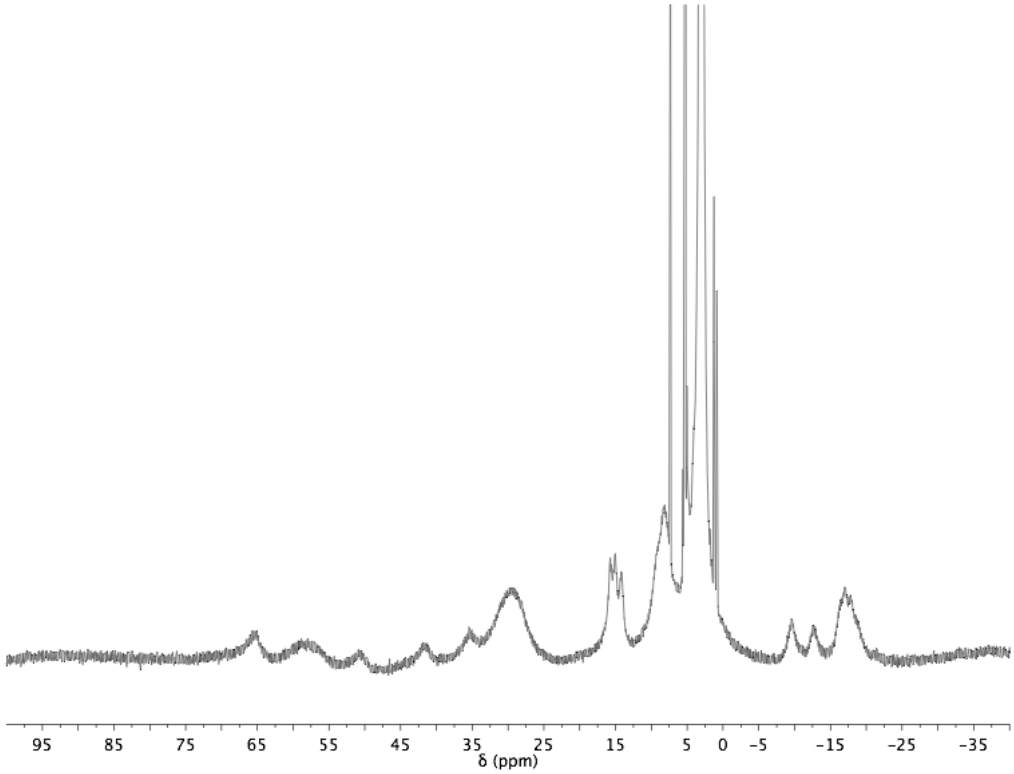

Figure S3. ^{1}H NMR spectrum of [**2**-Ca(DME)(OTf)]$^{+}$ in CD_2Cl_2 at 25 °C.

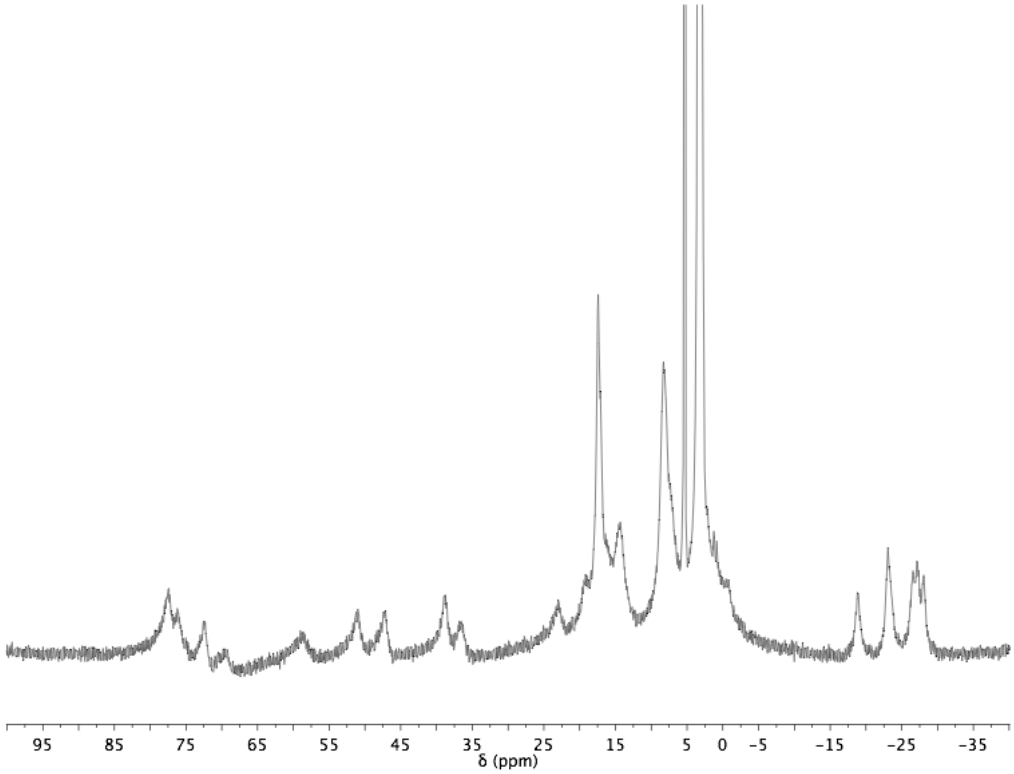

Figure S4. ^{1}H NMR spectrum of [**1**-Sr(DME)(OTf)]$^{2+}$ in CD_2Cl_2 at 25 °C.

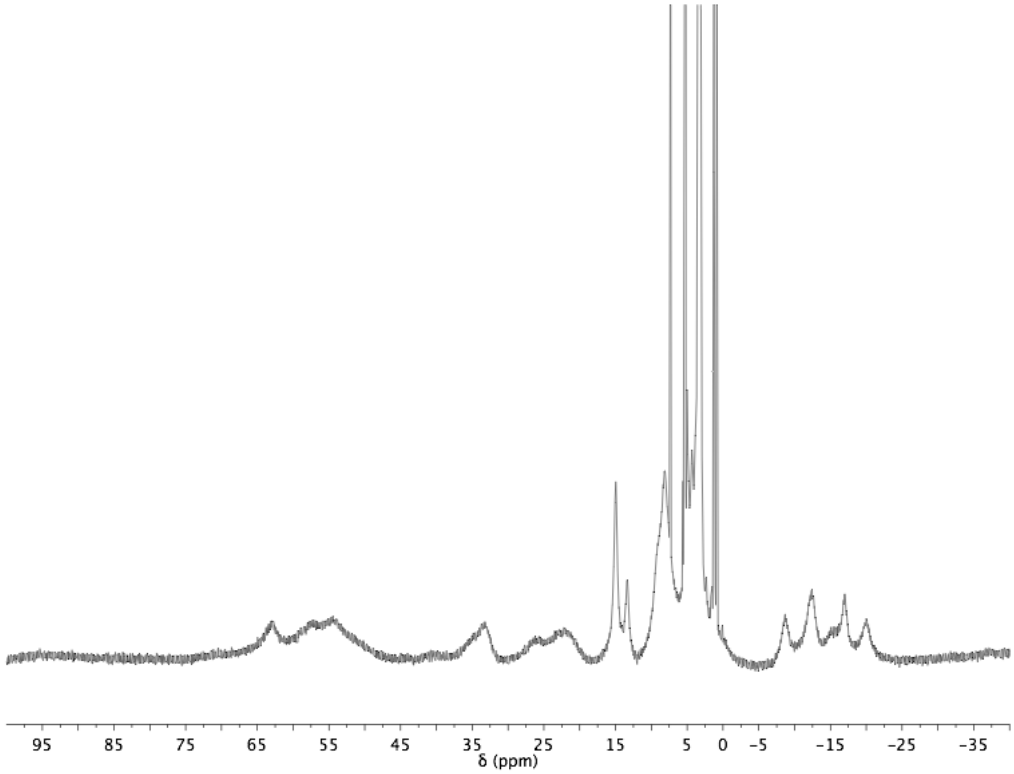

Figure S5. ^{1}H NMR spectrum of [**2**-Sr(DME)(OTf)]$^{+}$ in CD_2Cl_2 at 25 °C.

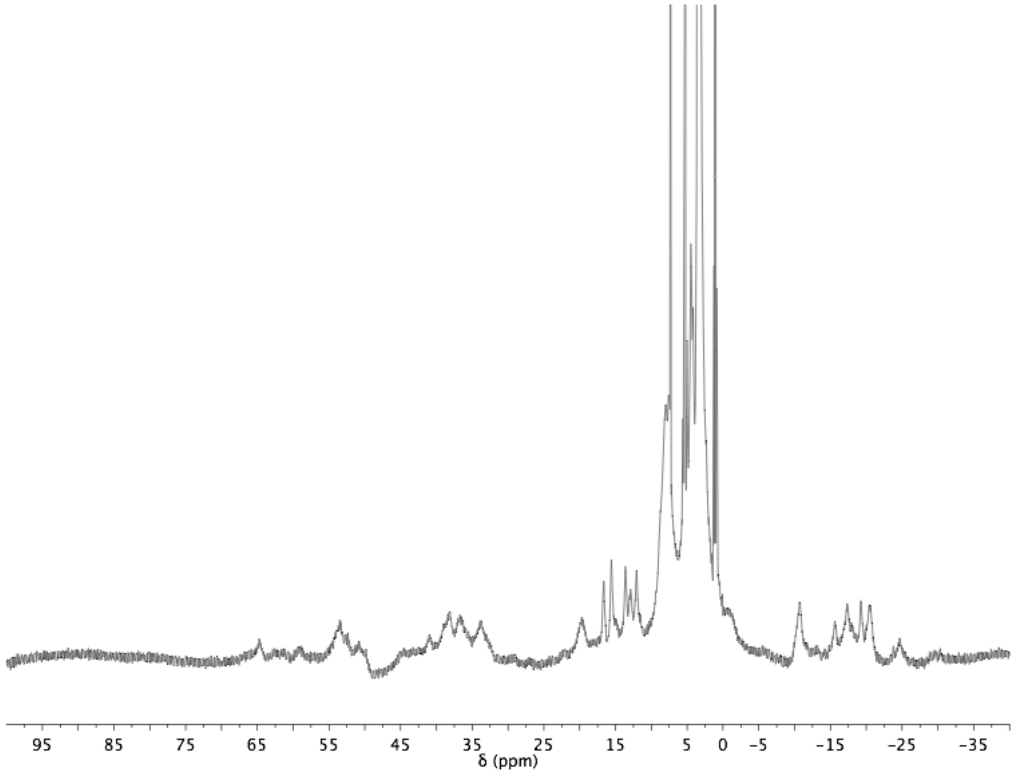

Figure S6. ^{1}H NMR spectrum of [**2**-Y(DME)(OTf)]$^{2+}$ in CD_2Cl_2 at 25 °C.

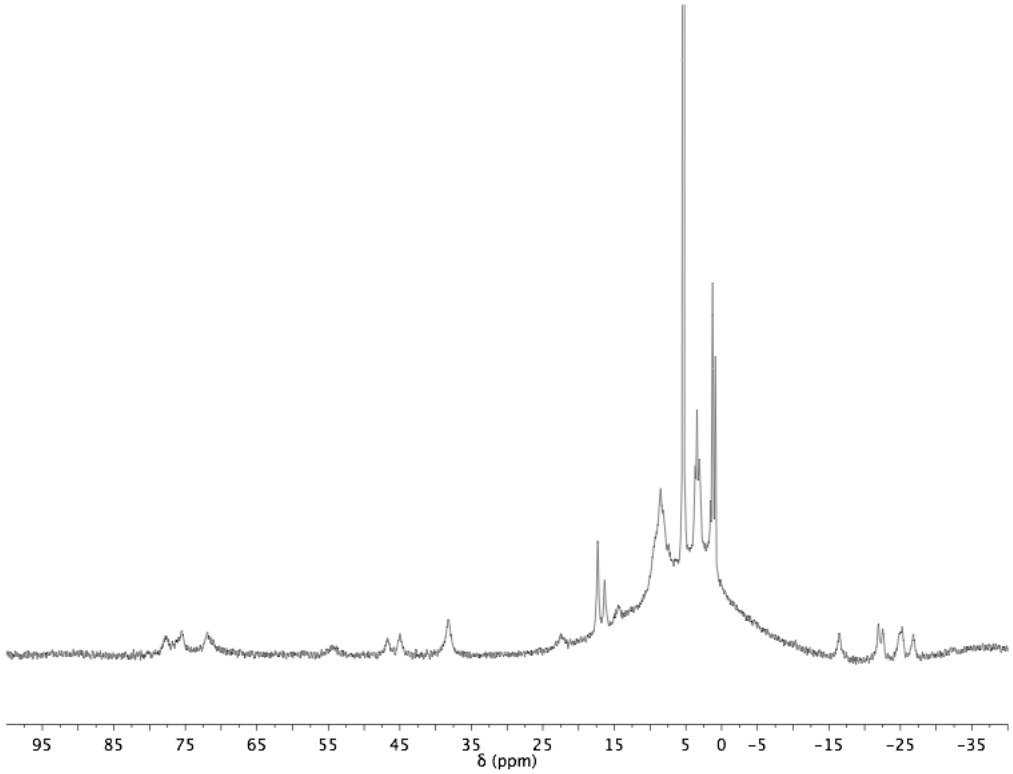

Figure S7. ^{1}H NMR spectrum of [**1**-Na]$_2^{4+}$ in CD_2Cl_2 at 25 °C.

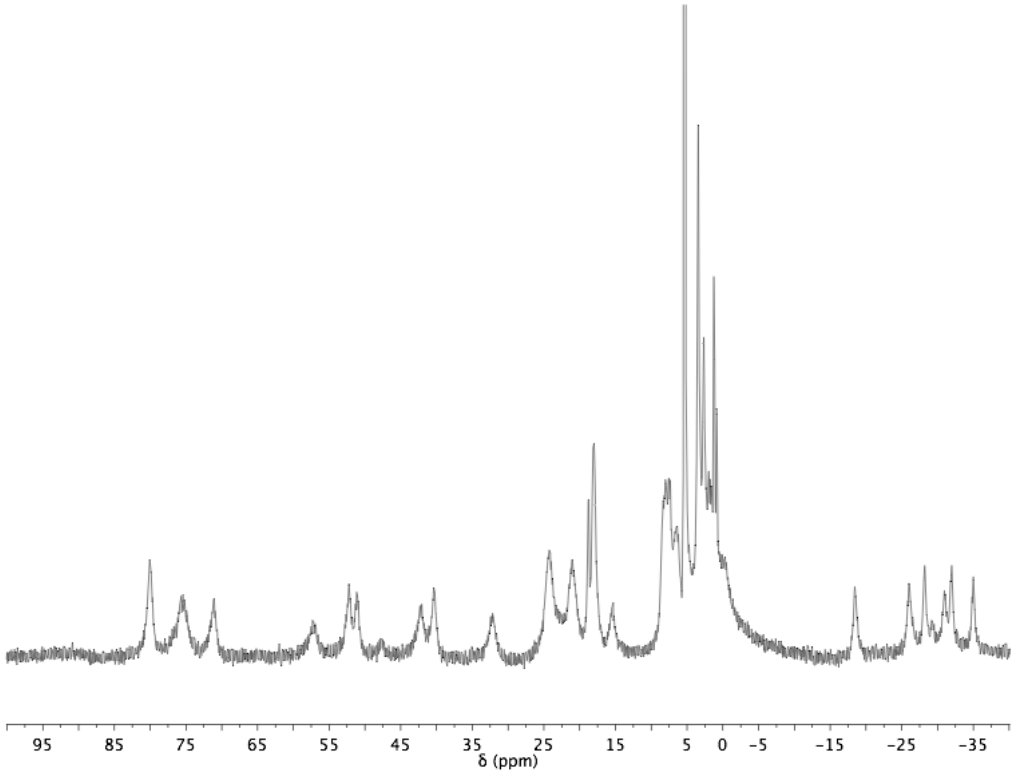

Figure S8. ^{1}H NMR spectrum of [**1**-Zn(CH_3CN)]$^{3+}$ in CD_2Cl_2 at 25 °C.

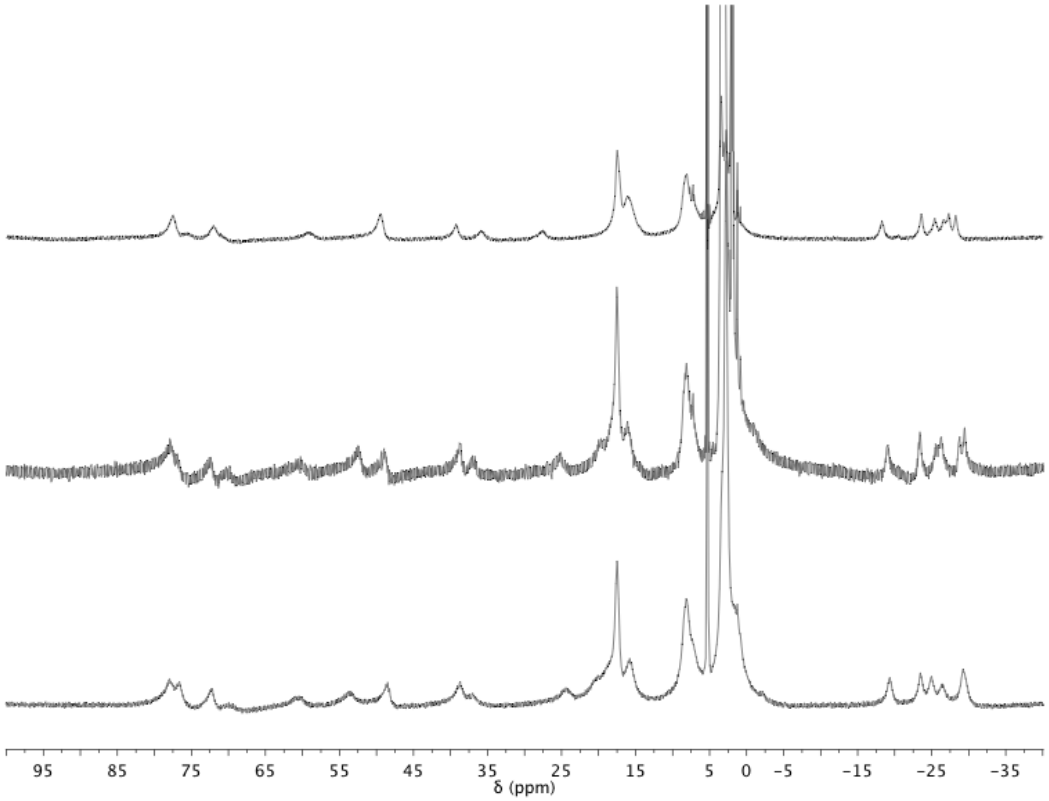

Figure S9. ^{1}H NMR spectra of CD_2Cl_2 solutions of [**1**-Ca$(H_2O)_3$]$^{3+}$ (top), [**1**-Ca$(H_2O)_3$]$^{3+}$ with added DME (middle), and [**1**-Ca(DME)(OTf)]$^{2+}$ (bottom) at 25 °C.

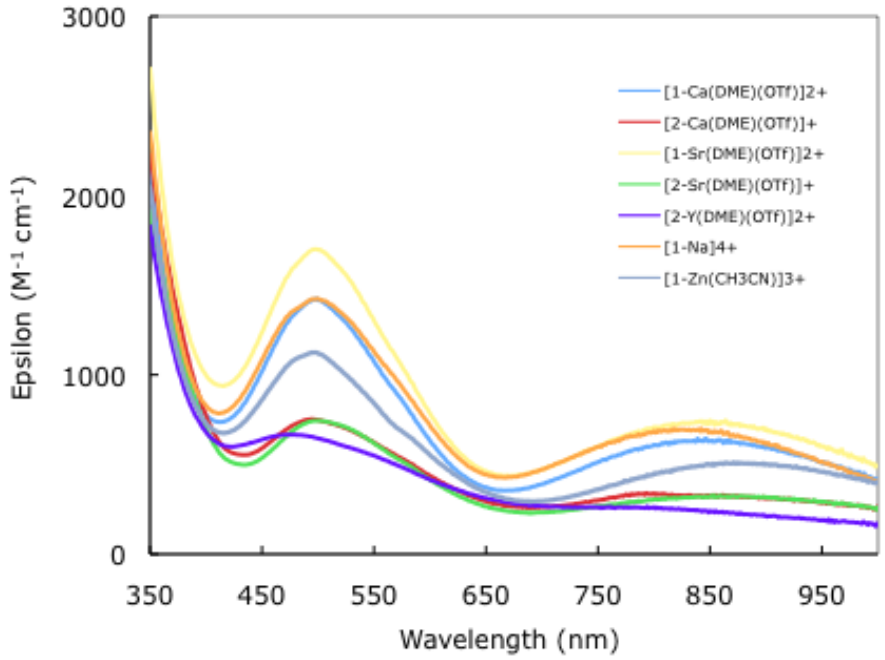

Figure S10. Electronic absorption spectra of trimanganese dioxo complexes in CH_2Cl_2 solution at room temperature.

Magnetic Susceptibility Measurements

General Considerations. DC magnetic susceptibility measurements were carried out in the Molecular Materials Research Center in the Beckman Institute of the California Institute of Technology on a Quantum Design MPMS instrument running MPMS MultiVu software. Powdered samples (0.038–0.056 g) were fixed in eicosane (0.05–0.11 g) in gelatin capsules and suspended in clear plastic straws. Data were recorded at 0.5 T from 4–300 K. Diamagnetic corrections were made using the average experimental magnetic susceptibility of **H_3L** at 0.5 T from 100–300 K (-593×10^{-6} cm^3/mol) in addition to the values of Pascal's constants for amounts of anion and solvent quantified for each sample using elemental analysis.

The $\chi_M T$ data taken at 0.5 T were fit to the magnetic susceptibility equation derived from the isotropic spin Hamiltonian for two coupling constants, J and J' [Eq. (1)].

$$\hat{H} = -2J[(\hat{S}_1 \bullet \hat{S}_2) + (\hat{S}_2 \bullet \hat{S}_3)] - 2J'(\hat{S}_3 \bullet \hat{S}_1) \quad (1)$$

The eigenvalues were determined using the Kambe method.[6] The data were fit from 10–300 K using Matlab[7] by minimizing $R = \sum \left| (\chi_M T)_{obs} - (\chi_M T)_{calcd} \right|^2 / \sum (\chi_M T)_{obs}{}^2$ (Table S1).

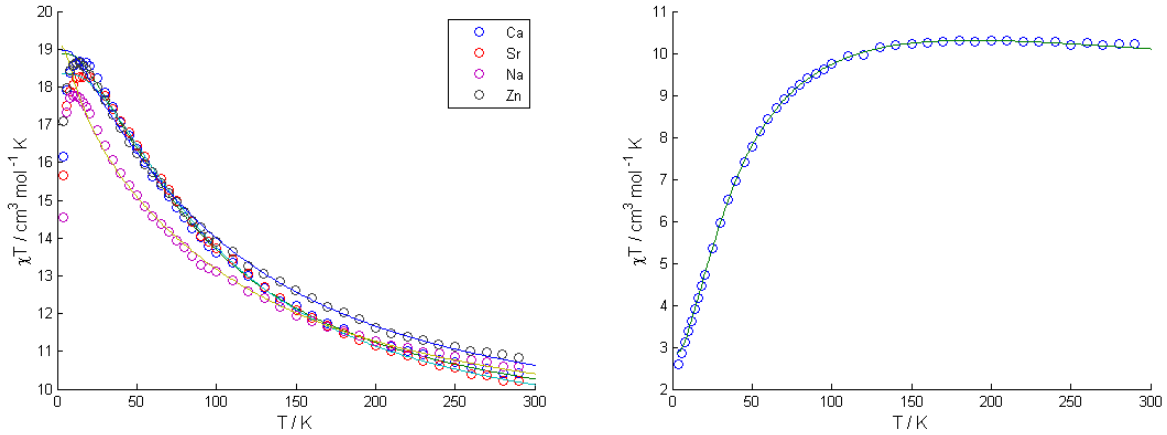

Figure S11. χ_MT vs. T data and fits for [**1**-Ca(DME)(OTf)][OTf]$_2$, [**1**-Sr(DME)(OTf)][OTf]$_2$, [**1**-Na]$_2$[OTf]$_4$, and [**1**-Zn(CH$_3$CN)][OTf]$_3$ (left), and χ_MT vs. T data and fit for [**2**-Ca(DME)(OTf)][OTf] (right). See Table S1 for fit parameters.

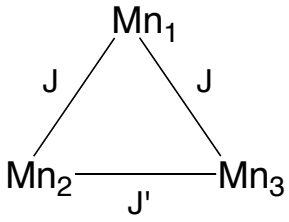

Figure S12. Exchange coupling model employed. For compounds **1**, the spins used were S = 3/2, 2, and 2 for Mn1, Mn2, and Mn3 respectively. For [**2**-Ca(DME)(OTf)][OTf)], the spins used were three S = 2 centers.

Table S1. Magnetic susceptibility fitting parameters.

Compound	Diamagnetic Correction ($\times 10^{-6}$ cm^3/mol)	J (cm^{-1})	J' (cm^{-1})	g	R ($\times 10^{-5}$)
[**1**-Ca(DME)(OTf)][OTf]$_2$	−938	12.9	−0.7	2.05	3.3
[**1**-Ca(DME)(OTf)][OTf]$_2$	−947	12.4	0.6	2.02	2.5
[**1**-Na]$_2$[OTf]$_4$	−715	17.3	−5.1	2.07	7.9
[**1**-Zn(CH$_3$CN)][OTf]$_3$	−715	17.3	−3.2	2.06	3.5
[**2**-Ca(DME)(OTf)][OTf]	−831	−2.3	25.3	1.95	1.7

Electrochemical Measurements

Electrochemical measurements were recorded with a Pine Instrument Company AFCBP1 bipotentiostat using the AfterMath software package.

Controlled-potential electrolysis was conducted in a sealed two-chambered H cell where the first chamber held the working and reference electrodes in 50 mL in 0.05 M LiOTf in 10:1 CH_2Cl_2/DME with ca. 0.5 mM of [**1**-Ca(DME)(OTf)][OTf]$_2$ (0.048 g, 0.027 mmol), and the second chamber held the auxiliary electrode in 25 mL of 0.05 M LiOTf in 10:1 CH_2Cl_2/DME. The two chambers were separated by a fine-porosity glass frit. Glassy carbon plates (12 cm × 3 cm × 1 cm; Tokai Carbon USA) were used as the working and auxiliary electrodes. The reference electrode was a Ag/Ag$^+$ NBu_4PF_6 in CH_3CN solution electrode separated from the solution by a Vycor frit. The cell was prepared and sealed in a nitrogen-filled glovebox before the beginning of the experiment. The experiment was run by holding the potential of the working electrode at −0.25 V vs. Ag/Ag$^+$ for 16 h until the current was nearly at 0 A. Integration of the current showed the passage of 2.06 C (0.8 electrons per molecule of [**1**-Ca(DME)(OTf)][OTf]$_2$). The purple solution in the first chamber was then removed from the cell and concentrated *in vacuo* to yield a purple solid that was taken up in CH_2Cl_2, filtered to remove excess LiOTf, then concentrated again. The ^{1}H NMR spectrum of a CD_2Cl_2 solution of the product matches that of [**2**-Ca(DME)(OTf)][OTf] in the presence of excess LiOTf (Figure S13). [**1**-Ca(DME)(OTf)][OTf]$_2$ does not react with LiOTf under the same conditions.

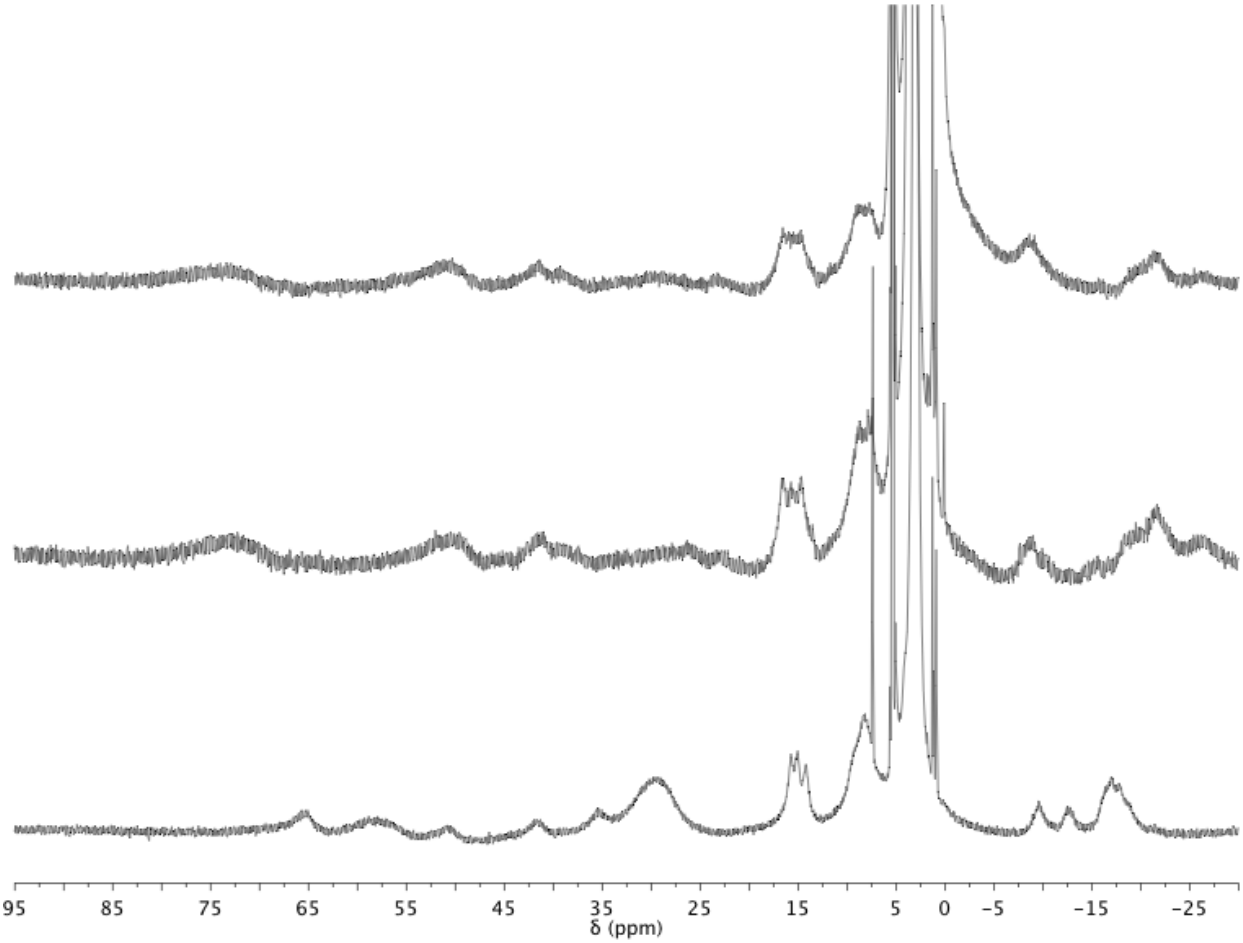

Figure S13. ^{1}H NMR spectra at 25 °C of CD_2Cl_2 solutions of the controlled-potential electrolysis product (top), [**2**-Ca(DME)(OTf)][OTf] after addition of LiOTf (middle), and [**2**-Ca(DME)(OTf)][OTf] (bottom).

Cyclic voltammograms were recorded on ca. 1 mM solutions of the relevant complexes in the glovebox at 20 °C with an auxiliary Pt-coil electrode, a Ag/Ag+ reference electrode (0.01 M $AgNO_3$, 0.1 M $^{n}Bu_4NPF_6$ in CH_3CN), and a 3.0 mm glassy carbon electrode disc (BASI). The electrolyte solutions were 0.1 M $^{n}Bu_4NPF_6$ in CH_2Cl_2 ([**1**-Na]$_2^{4+}$) or 10:1 CH_2Cl_2/DME ([**1**-Ca(DME)(OTf)]$^{2+}$, [**1**-Sr(DME)(OTf)]$^{2+}$, [**1**-Zn(CH_3CN)]$^{3+}$, and [**2**-Y(DME)(OTf)]$^{2+}$). For [**1**-Ca(DME)(OTf)]$^{2+}$, [**1**-Sr(DME)(OTf)]$^{2+}$, and [**1**-Na]$_2^{4+}$, CVs were also recorded in an electrolyte solution of 0.1 M $^{n}Bu_4NPF_6$ in CH_2Cl_2 using a hanging mercury drop electrode (BASI CGME). Using the average mass of the mercury drop (0.037 g), the surface area of the drop (assumed to be a sphere) was calculated to be 0.095 cm^2. All reported values are referenced to an internal ferrocene/ferrocenium couple.

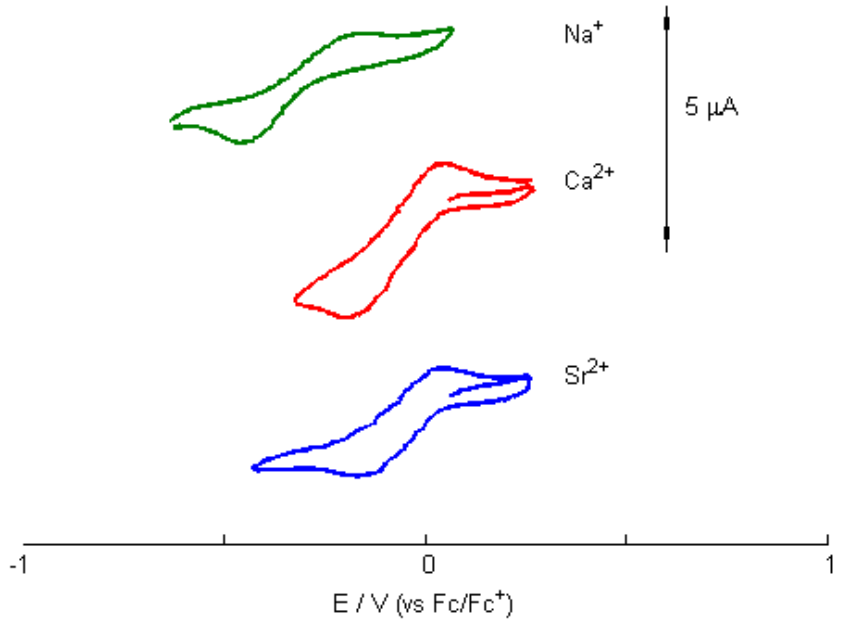

Figure S14. Cyclic voltammograms of complexes using a hanging mercury drop electrode at 20 °C at a scan rate of 100 mV/s. Each redox event corresponds to the $[MMn^{IV}Mn^{III}_2O_2]/[MMn^{III}_3O_2]$ couple referenced to an internal Fc/Fc^+ standard.

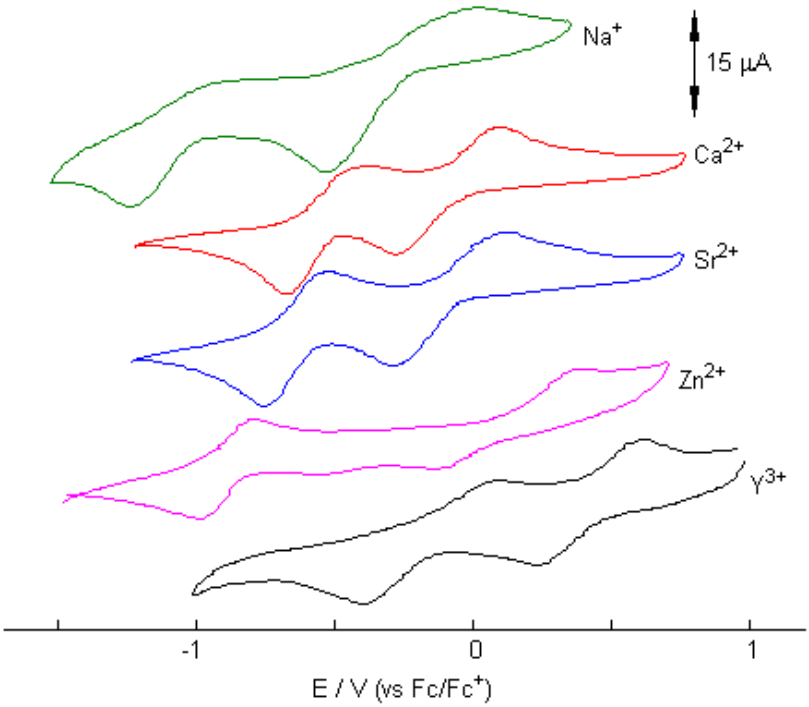

Figure S15. Cyclic voltammograms of complexes using a GCE at 20 °C showing both redox events. CVs were taken at a scan rate of 100 mV/s and referenced to an internal Fc/Fc^+ standard.

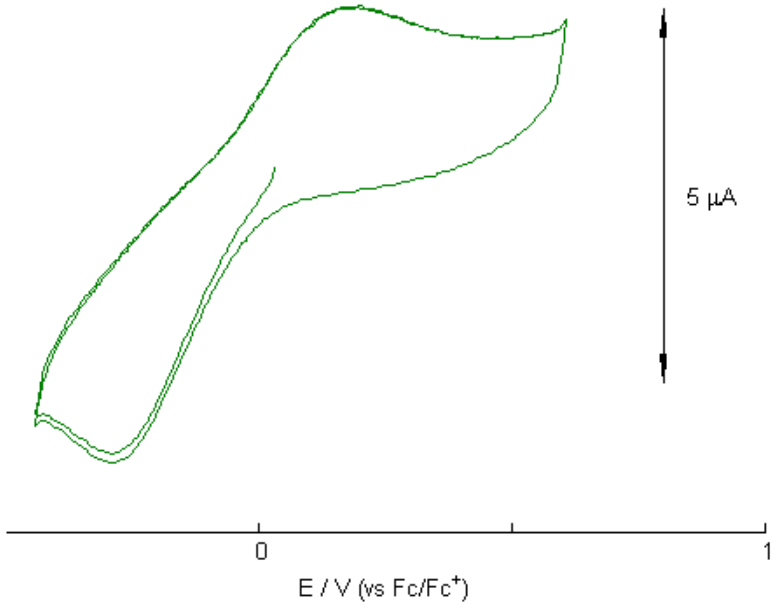

Figure S16. Cyclic voltammogram of a solution of [**1**-Ca(H_2O)$_3$]$^{3+}$ in 0.1 M NBu_4PF_6 in 10:1 CH_2Cl_2/DME at a scan rate of 50 mV/s using a GCE. $E_{1/2}$ = –0.05 V vs. Fc/Fc$^+$.

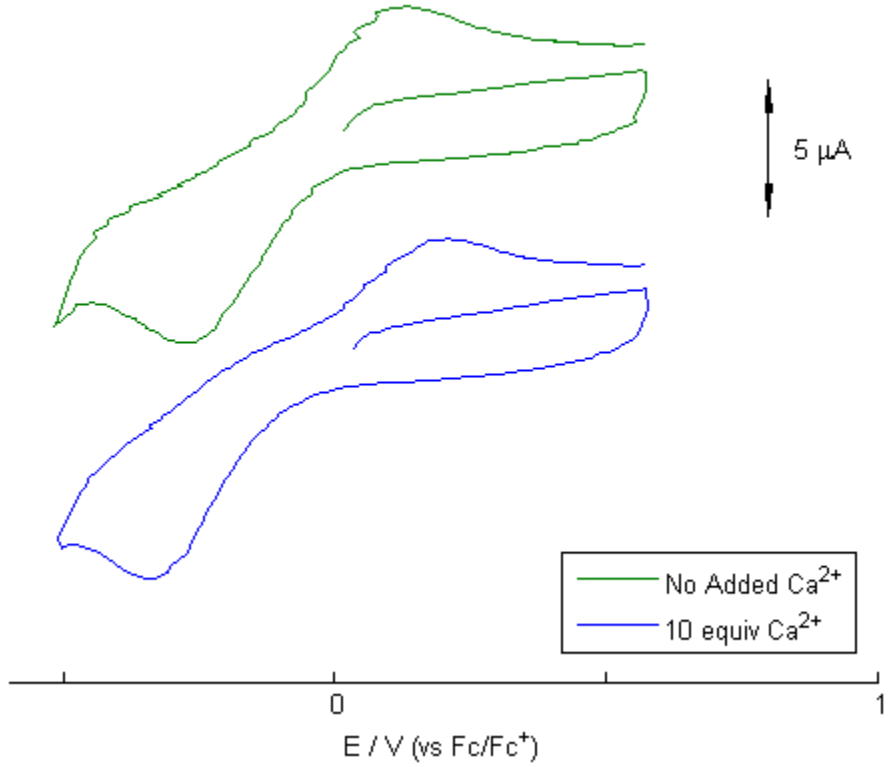

Figure S17. Cyclic voltammograms at 100 mV/s using a GCE in 0.1 M NBu_4PF_6 in 10:1 CH_2Cl_2/DME of [**1**-Ca(DME)(OTf)]$^{2+}$ (green) and [**1**-Ca(DME)(OTf)]$^{2+}$ with 10 equivalents of Ca(OTf)$_2$ (blue). $E_{1/2}$ = –0.07 V vs. Fc/Fc$^+$ for both voltammograms.

Table S2. $E_{1/2}$ values of the $[MMn_3O_2]^{n+6}/[MMn_3O_2]^{n+5}$ couple vs. Fc/Fc^+ using the glassy carbon electrode (GCE) and the hanging mercury drop electrode.

M	GCE (V)	Hg (V)
Na	–0.30	–0.31
Sr	–0.07	–0.06
Ca	–0.07	–0.07
Zn	0.16	--
Y	0.42	--

Spectral Redox Titration

The titration procedures were based off of published methods.[8] Electron transfer from dimethylferrocene to [**1**-Ca(DME)(OTf)]$^{2+}$ (6.2×10^{-4} M) and from [**2**-Ca(DME)(OTf)]$^+$ to dimethylferrocenium triflate was measured from the spectral change in the presence of various concentrations of dimethylferrocene ($4.8 \times 10^{-4} – 1.9 \times 10^{-3}$ M) at 298 K (Figure S18) using a Cary 50 spectrophotometer with quartz cuvettes sealed with Teflon stoppers (path length = 10 mm). In a glovebox, a solution of dimethylferrocene in 10:1 CH_2Cl_2/DME was added via a microsyringe to a solution of [**1**-Ca(DME)(OTf)]$^{2+}$ in 10:1 CH_2Cl_2/DME (3 mL). The concentrations of [**1**-Ca(DME)(OTf)]$^{2+}$, [**2**-Ca(DME)(OTf)]$^+$, dimethylferrocene, and dimethylferrocenium triflate were determined by spectral deconvolution using Matlab.

The equilibrium constant (K_{et}) of eq. 2 was determined by fitting the plot in Figure S19 to then yield the E_{red} value of the reduction of [**1**-Ca(DME)(OTf)]$^{2+}$ vs. the E_{ox} of dimethylferrocene from eq. 3.[8] The reduction potential vs. Fc/Fc^+ was determined by subtracting 90 mV.

$$Me_2Fc + [\mathbf{1}\text{-Ca(DME)(OTf)}]^{2+} \overset{K_{et}}{\rightleftharpoons} Me_2Fc^+ + [\mathbf{2}\text{-Ca(DME)(OTf)}]^+ \quad (2)$$

$$E_{red} = E_{ox} + (RT/F) \ln K_{et} \quad (3)$$

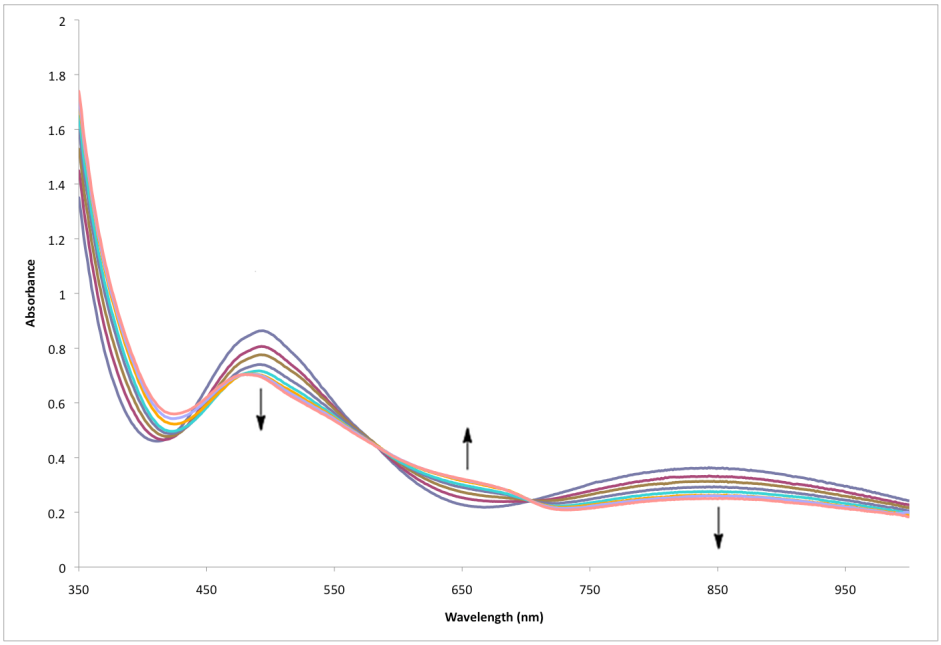

Figure S18. Spectral changes observed in electron transfer from dimethylferrocene to [**1**-Ca(DME)(OTf)]$^{2+}$ in 10:1 CH_2Cl_2/DME at 298 K.

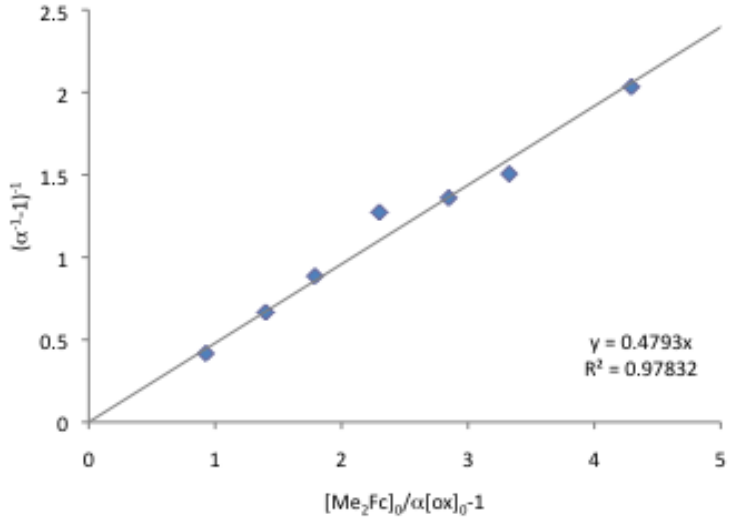

Figure S19. Plot of $(\alpha^{-1} - 1)^{-1}$ vs. $[Me_2Fc]_0/\alpha[[\mathbf{1}\text{-Ca(DME)(OTf)}]^{2+}]_0 - 1$ (See ref. 8 for details). The calculated $K_{et} = 0.48$, corresponding to $E_{1/2}$ of –0.11 vs. Fc/Fc^+.

The $E_{1/2}$ of the [**1**-Ca(DME)(OTf)]$^{2+}$/[**2**-Ca(DME)(OTf)]$^+$ couple was also determined by titrating a 10:1 CH_2Cl_2/DME solution of [**2**-Ca(DME)(OTf)]$^+$ (6.1×10^{-4} M) with dimethylferrocenium triflate (8.6×10^{-5} – 1.3×10^{-3} M) (Figure S20). By fitting the reverse reaction of eq. 1 in the same manner as above (Figure S21), the E_{ox} of [**2**-Ca(DME)(OTf)]$^+$ vs. the E_{red} of dimethylferrocenium triflate was calculated from the K_{et}.

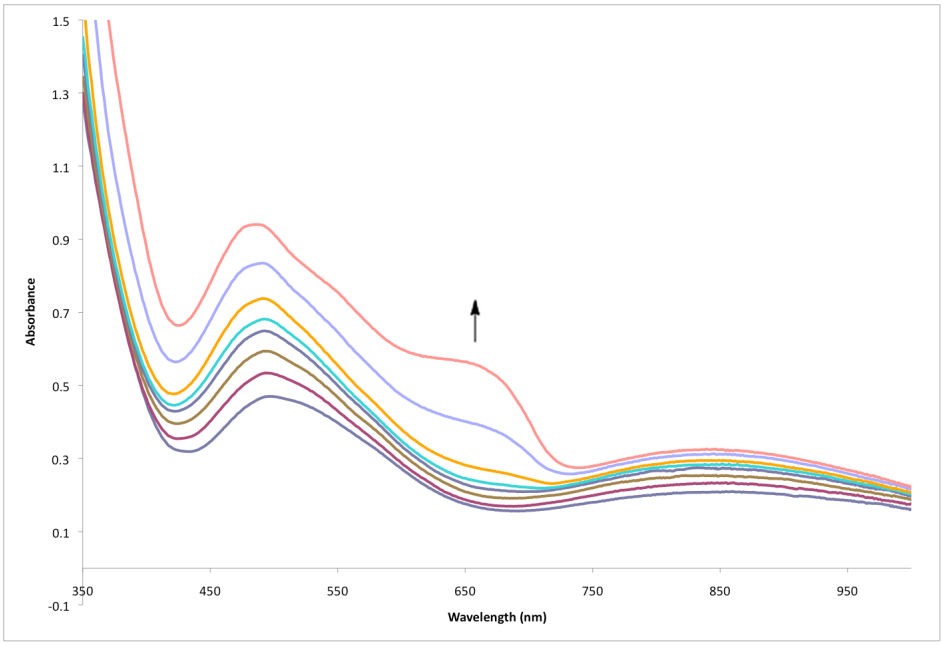

Figure S20. Spectral changes observed in electron transfer from [**2**-Ca(DME)(OTf)]$^+$ to dimethylferrocenium triflate in 10:1 CH_2Cl_2/DME at 298 K.

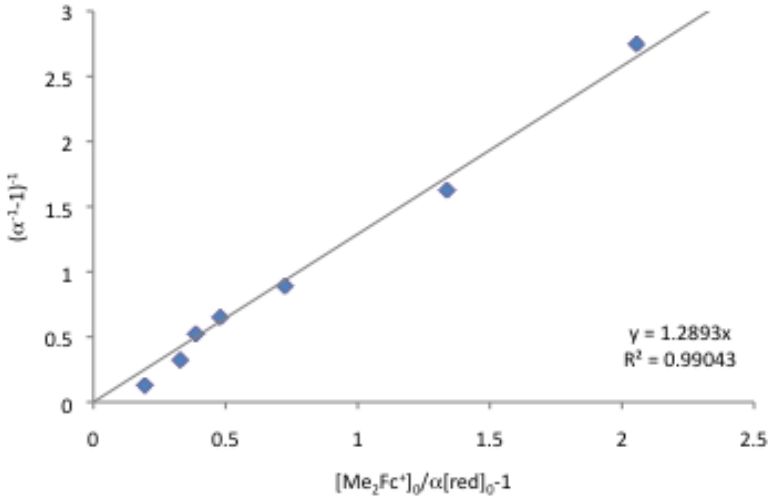

Figure S21. Plot of $(\alpha^{-1} - 1)^{-1}$ vs. $[Me_2Fc^+]_0/\alpha[[\mathbf{2}\text{-Ca(DME)(OTf)}]^+]_0 - 1$ (See ref. 8 for details). The calculated K_{et} = 1.3, corresponding to $E_{1/2}$ of –0.10 vs. Fc/Fc^+.

^{18}O Labeling Studies

ESI-MS Procedures

In a nitrogen glovebox, samples were dissolved in dry CH_2Cl_2 (ca. 10 μM) in 1.5 mL snap-cap vials. The line and inlet of the instrument were rinsed with dry CH_2Cl_2 before injecting the sample. Spectra were collected by averaging 70 or more scans. The fragment analyzed was that of $[LCaMn_3{}^{16}O_2(OAc)(OTf)_2]^+$. MS calcd. for $C_{61}H_{42}CaF_6Mn_3N_6O_{13}S_2$ (M^+): 1448.99.

Synthesis of ^{18}O-labeled [1*-Ca(DME)(OTf)][OTf]$_2$

In a glovebox, a scintillation vial equipped with a stir bar was charged with $LMn_3(OAc)_3$ (0.050 g, 0.0418 mmol), $Ca(OTf)_2$ (0.021 g, 0.0627 mmol, 1.5 equiv), and DME (5 mL). After stirring for 2 min., $PhI^{18}O$ (0.019 g, 0.0835 mmol, 2 equiv)[9] was added as a solid, and the mixture was stirred for 2 h at room temperature, becoming a purple mixture. The purple precipitate was collected over Celite, then extracted with CH_2Cl_2 to yield the product as a red-purple solid (0.031 g, 42%). The ^{1}H NMR spectrum matches that of unlabeled [**1**-Ca(DME)(OTf)][OTf]$_2$. The isotopic enrichment is approximately 9:49:41 ($^{16}O_2/^{16}O^{18}O/^{18}O_2$) (Figure S22, Table S3).

Crossover Experiment

In a glovebox, a scintillation vial equipped with a stir bar was charged with [**1**-Ca(DME)(OTf)][OTf]$_2$ (0.005 g, 0.003 mmol) and [**1***-Ca(DME)(OTf)][OTf]$_2$ (0.005 g, 0.003 mmol). Dichloromethane (5 mL) was added. Aliquots were taken of the reaction mixture at 1 min. and 1 h, diluted with dichloromethane, and measured by ESI-MS. Relative isotopic amounts were calculated using Matlab[7] and the expected isotopic ratios of clean species.

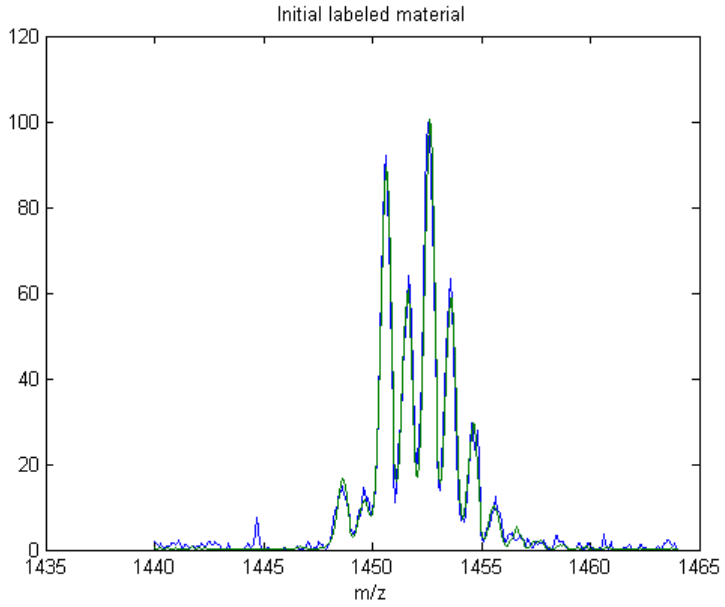

Figure S22. ESI-MS of a CH_2Cl_2 solution of [**1***-Ca(DME)(OTf)][OTf]$_3$ (blue) and theoretical spectrum of mixture of isotopologs (green).

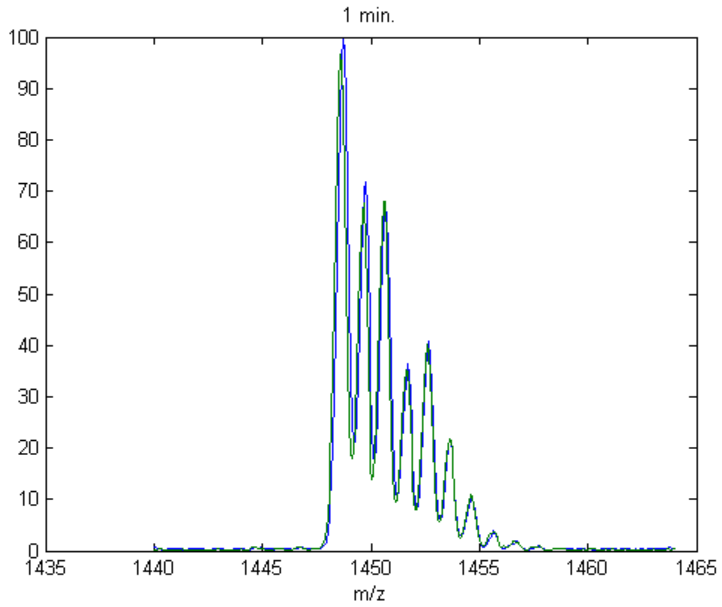

Figure S23. ESI-MS of a CH_2Cl_2 solution of a ca. 1:1 mixture of [**1**-Ca(DME)(OTf)]$^{2+}$ and [**1***-Ca(DME)(OTf)]$^{2+}$ after 1 min (blue) and theoretical spectrum from calculated isotopolog ratios (green).

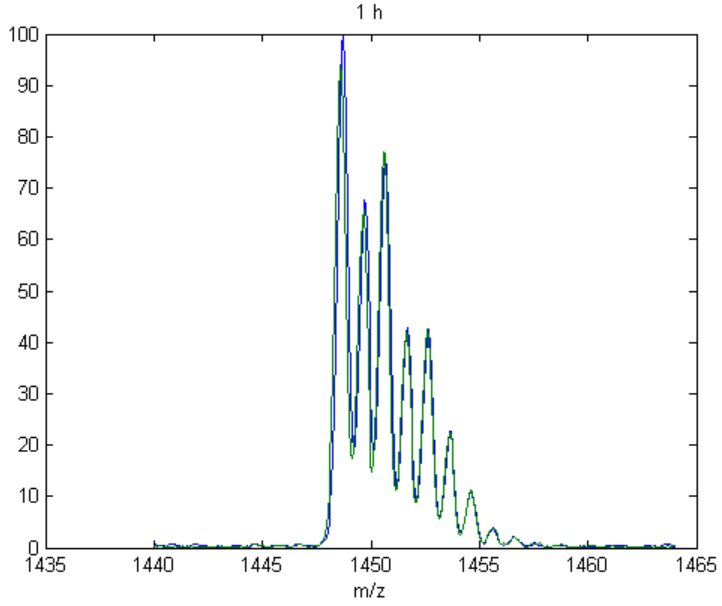

Figure S24. ESI-MS of a CH_2Cl_2 solution of a ca. 1:1 mixture of [**1**-Ca(DME)(OTf)]$^{2+}$ and [**1***-Ca(DME)(OTf)]$^{2+}$ after 1 h (blue) and theoretical spectrum from calculated isotopolog ratios (green).

Table S3. Ratios of isotopologs of [**1**-Ca(DME)(OTf)]$^{2+}$ and calculated amount of ^{18}O-mixing.

	Percent $^{16}O_2$	Percent $^{16}O^{18}O$	Percent $^{18}O_2$	% Crossover
Initial **1***	9.3	49.3	41.4	0
1 min.[a]	62.8	22.5	14.6	7
1 h[a]	58.6	27.8	13.6	18

[a] Ratios were calculated based upon mass spectrometry data of aliquots of a ca. 1:1 mixture of [**1**-Ca(DME)(OTf)]$^{2+}$ and [**1***-Ca(DME)(OTf)]$^{2+}$ taken at the indicated time points.

Crystallographic Information

CCDC 898246–898252 and 906249 contain the supplementary crystallographic data for this paper. These data can be obtained free of charge from The Cambridge Crystallographic Data Centre via www.ccdc.cam.ac.uk/data_request/cif.

Refinement details

In each case, crystals were mounted on a glass fiber or nylon loop using Paratone oil, then placed on the diffractometer under a nitrogen stream. Low temperature (100 K) X-ray data were obtained on a Bruker APEXII CCD based diffractometer (Mo sealed X-ray tube, K_α = 0.71073 Å). All diffractometer manipulations, including data collection, integration and scaling were carried out using the Bruker APEXII software.[10] Absorption corrections were applied using SADABS.[11] Space groups were determined on the basis of systematic absences and intensity statistics and the structures were solved by direct methods using XS[12] (incorporated into SHELXTL) and refined by full-matrix least squares on F^2. All non-hydrogen atoms were refined using anisotropic displacement parameters. Hydrogen atoms were placed in idealized positions and refined using a riding model. The structure was refined (weighted least squares refinement on F^2) to convergence.

It should be noted that due to the size of these compounds, most crystals included solvent accessible voids, which tended to contain disordered solvent. In addition, due to a tendency to desolvate, the long range order of these crystals and amount of high angle data we were able to record was in some cases not ideal. These disordered solvent molecules were largely responsible for the alerts generated by the checkCIF protocol. In some cases, this disorder could be modeled satisfactorily, while in two ([**1**-Ca$(H_2O)_3$](OTf)$_3$ and [**2**-Y(DME)(OTf)](OTf)$_2$), the disordered solvent was removed using the SQUEEZE protocol included in PLATON[13] (*vide infra*). In all cases, we are confident this additional electron density is attributable to solvent included in the crystal lattice and not unaccounted for counterions. Refinement details for each compound are included below.

Table S4. Crystal and refinement data.

	[1-Ca(DME)(OTf)](OTf)$_2$	**[1-Ca(H$_2$O)$_3$](OTf)$_3$**	**[2-Ca(DME)(OTf)](OTf)**	**[1-Sr(DME)(OTf)](OTf)$_2$**	**[2-Sr(DME)(OTf)](OTf)**	**[1-Zn(CH$_3$CN)](OTf)$_3$**	**[1-Na]$_2$(OTf)$_4$**	**[2-Y(DME)(OTf)](OTf)$_2$**
empirical formula	$C_{68}H_{55}CaF_9Mn_3N_6O_{20}S_3$	$C_{64}H_{45}CaF_9Mn_3N_6O_{21}S_3$	$C_{76}H_{65}CaF_6Mn_3N_6O_{19}S_2$	$C_{75}H_{57}Cl_2F_9Mn_3N_6O_{20}S_3Sr$	$C_{76}H_{65}F_6Mn_3N_6O_{19}S_2Sr$	$C_{67.40}H_{47.11}F_9Mn_3N_{7.70}O_{18}S_3Zn$	$C_{126}H_{90}F_{12}Mn_6N_{12}Na_2O_{31.74}S_4$	$C_{72}H_{65}F_9Mn_3N_6O_{21}S_3Y$
formula wt	1748.26	1706.14	1749.36	1952.79	1796.90	1750.21	3011.80	1871.21
T (K)	100	100	100	100	100	100	100	100
a, Å	13.5027(13)	14.7053(8)	11.6790(4)	16.0744(8)	11.7071(4)	14.3484(8)	13.5641(16)	14.7253(17)

b, Å	19.1805(17)	14.7735(8)	27.0308(9)	26.0588(13)	27.1019(12)	14.3923(7)	15.0073(17)	25.280(3)
c, Å	27.433(3)	18.508(1)	25.7452(9)	20.2364(11)	25.4494(11)	18.5632(9)	16.813(2)	23.717(3)
α, deg	90	69.988(3)	90	90	90	72.643(3)	102.848(4)	90
β, deg	91.337(4)	72.802(3)	93.682(2)	105.055(3)	93.564(2)	73.273(3)	109.783(4)	102.212(6)
γ, deg	90	69.910(2)	90	90	90	70.956(3)	93.581(4)	90
V, Å^3	7102.9(11)	3475.2(3	8110.8(5)	8185.7(7)	8059.1(6)	3380.7(3)	3104.2(6)	8629.1(17)
Z	4	2	4	4	4	2	1	4
cryst syst	Monoclinic	Triclinic	Monoclinic	Monoclinic	Monoclinic	Triclinic	Triclinic	Monoclinic
space group	P2(1)/c	P-1	P2(1)/c	P2(1)/n	P2(1)/c	P-1	P-1	P2(1)/c
d_{calcd}, g/cm^3	1.635	1.630	1.433	1.585	1.481	1.719	1.611	1.440
θ range, deg	1.83–27.03	1.20–27.50	1.75–32.34	1.65–27.50	1.70–25.00	1.54–27.50	1.98–24.00	1.63–27.50
μ, mm^{-1}	0.788	0.804	0.659	1.336	1.255	1.096	0.769	1.256
abs cor	Semi-empirical from equivalents	Semi-empirical from equivalents	Semi-empirical from equivalents	Semi-empirical from equivalents	Semi-empirical from equivalents	Semi-empirical from equivalents	Semi-empirical from equivalents	Semi-empirical from equivalents
GOF[c]	1.901	1.669	1.351	1.683	1.110	1.466	1.434	1.070
R1,[a] wR2[b] ($I > 2\sigma(I)$)	0.0647, 0.0834	0.0516, 0.1732	0.0939, 0.2338	0.1018, 0.3081	0.0865, 0.1959	0.0694, 0.2015	0.0711, 0.1588	0.0515, 0.1233

[a] $R1 = \Sigma||F_o|-|F_c|| / \Sigma|F_o|$ [b] $wR2 = \{ \Sigma [w(F_o^2-F_c^2)^2] / \Sigma [w(F_o^2)^2] \}^{1/2}$ [c] $GOF = S = \{ \Sigma [w(F_o^2-F_c^2)^2] / (n-p) \}^{1/2}$

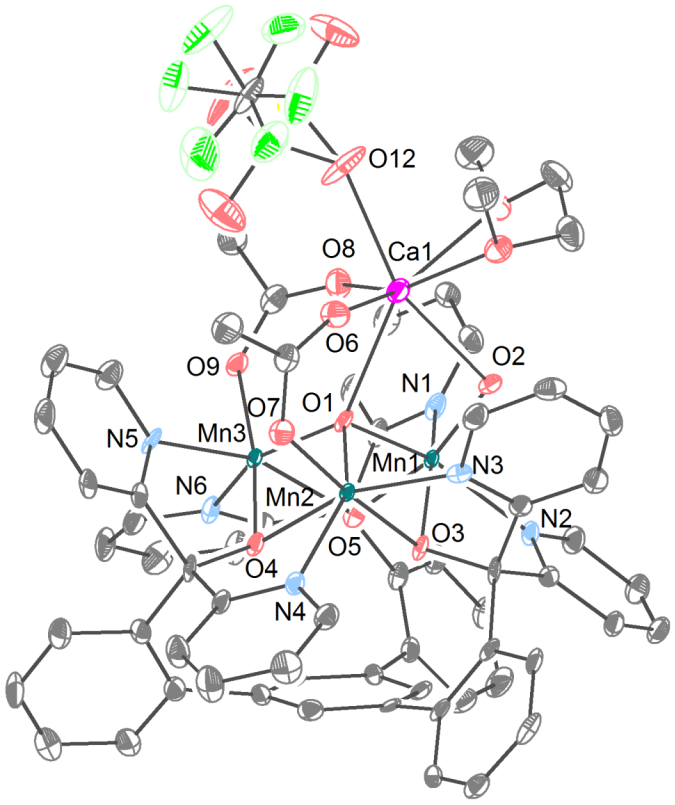

Figure S25. Structural drawing of [**1**-Ca(DME)(OTf)](OTf)$_2$ with 50% probability ellipsoids. Outer-sphere trifluoromethanesulfonate ions and hydrogen atoms not shown for clarity.

Special refinement details for [1-Ca(DME)(OTf)](OTf)$_2$
The structure contains a disordered trifluoromethanesulfonate counterion bound to the calcium center. Restraints and populations were employed to model this anion in two positions. Additionally, restraints were employed to treat the displacement parameters of some of the carbons to acceptable sizes. Crystals of this compound were weakly diffracting and had very little high angle data. The present data and solution represent the best of a number of data collections using different crystals. The CIF file and CheckCIF file output contain validation reply form items which address this issue.

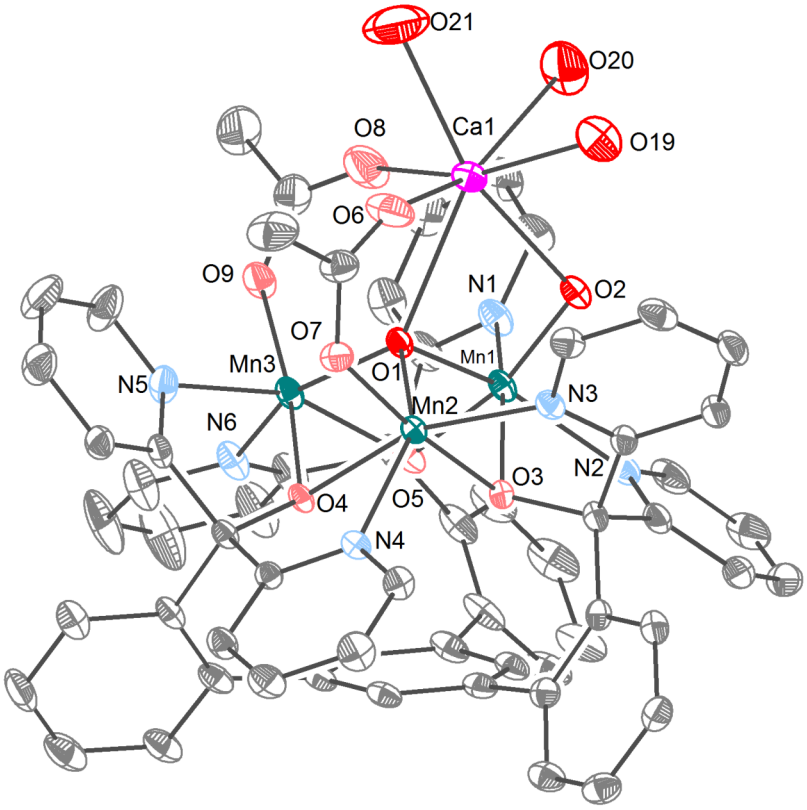

Figure S26. Structural drawing of [**1**-Ca(H_2O)$_3$](OTf)$_3$ with 50% probability ellipsoids. Outer-sphere trilfuoromethanesulfonate anions and hydrogen atoms not pictured for clarity.

Special refinement details for [1-Ca(H_2O)$_3$](OTf)$_3$
The structure contains three water ligands coordinated to the calcium center, for which hydrogen atoms were not modelled. Three outer-sphere trifluoromethanesulfonate atoms were located. The crystal also contains other disordered solvent molecules, presumably dichloromethane (present in the crystallization) that could not be satisfactorily modeled. SQUEEZE was employed to produce a bulk solvent correction to the observed intensities. The program accounted for 68 electrons.

This is in reasonable agreement with what would be expected for two disordered molecules of dichloromethane (84 electrons).

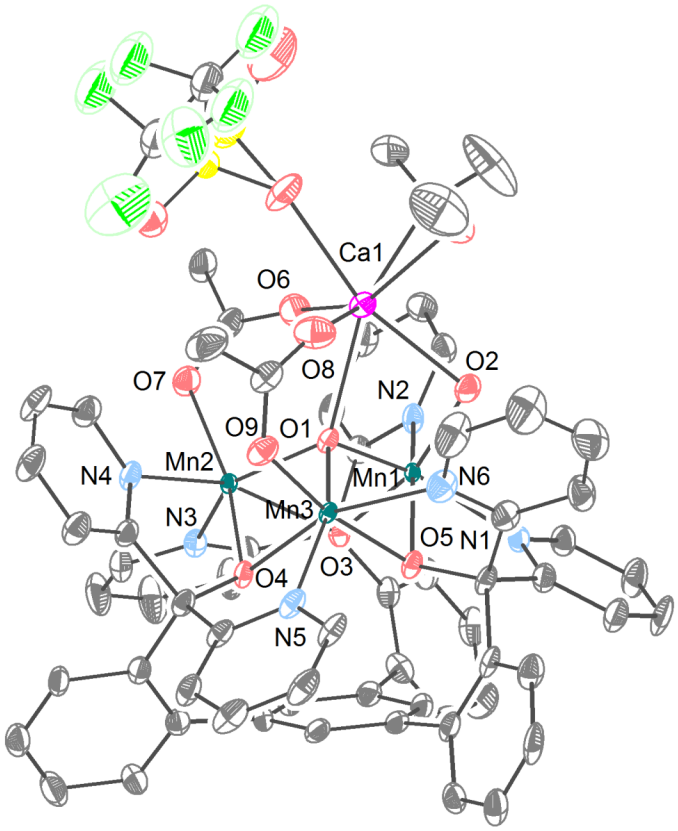

Figure S27. Structural drawing of [**2**-Ca(DME)(OTf)](OTf) with 50% probability ellipsoids. Outer-sphere trifluoromethanesulfonate ions and hydrogen atoms not shown for clarity.

Special refinement details for [2-Ca(DME)(OTf)](OTf)

The structure contains a disordered trifluoromethanesulfonate ion bound to the calcium center, and populations were employed to model the ion in two positions. Restraints were used to treat the distances, angles, and displacement parameters of the counterion. The crystal also contains some disordered solvent, which was constrained as a pentane molecule in two positions, but may also be a more disordered 1,2-dimethoxyethane molecule (both solvents were present in the crystallization mixture). We were unable to rule out one or the other due to the severe disorder. Restraints were employed to treat the displacement parameters of this disordered solvent and of the disordered triflate ion to acceptable sizes. The crystal also contains another 1,2-dimethoxyethane molecule that is not disordered and presents satisfactory thermal parameters.

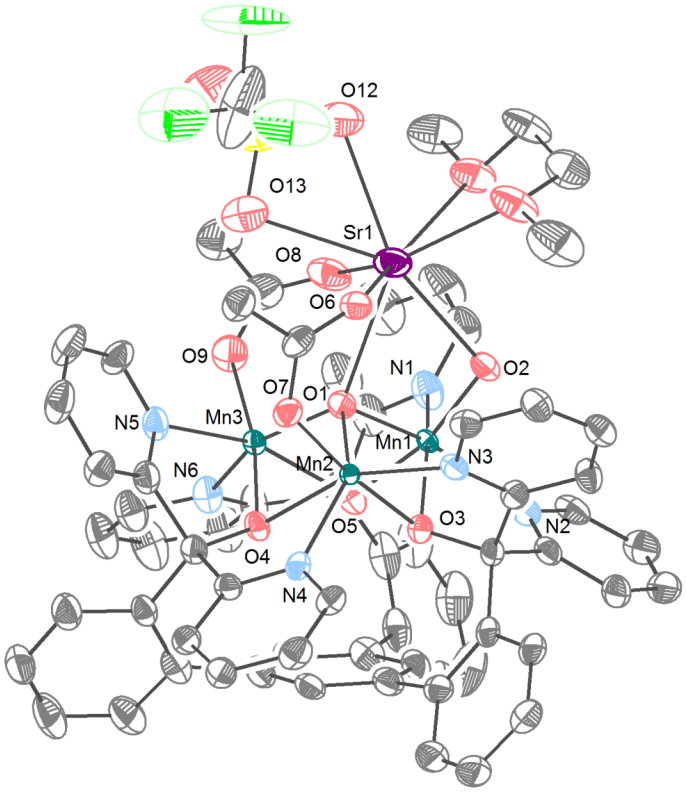

Figure S28. Structural drawing of [**1**-Sr(DME)(OTf)](OTf)$_2$ with 50% probability ellipsoids. Outer-sphere trifluoromethanesulfonate ions and hydrogen atoms not shown for clarity.

Special refinement details for [1-Sr(DME)(OTf)](OTf)$_2$

The structure contains a disordered dichloromethane molecule, which was refined by modeling two positions and constraining the bond distances and angles. Restraints were employed to treat the displacement parameters of this disordered dichloromethane to acceptable sizes. The crystal also contains a disordered solvent molecule which was constrained as a hexane molecule with restrained displacement parameters. Both dichloromethane and hexanes were present as crystallization solvents. The final refined R1 value is high (0.102) due to the large amount of solvent disorder, leading to loss of long range order and poor diffraction of the small crystal, but these data were the best collected from collection of multiple crystals.

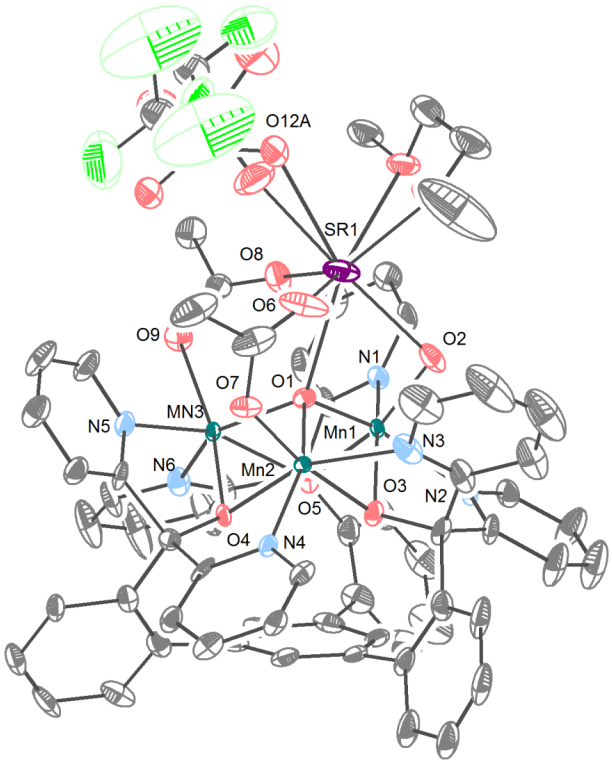

Figure S29. Structural drawing of [**2**-Sr(DME)(OTf)](OTf) with 50% probability ellipsoids. Outer-sphere trifluoromethanesulfonate ions and hydrogen atoms not shown for clarity.

Special refinement details for [2-Sr(DME)(OTf)](OTf)

The structure contains a disordered trifluoromethanesulfonate counterion bound to strontium, which was modeled in two positions using populations. Restraints were employed to treat the distances, angles, and displacement parameters of this disordered counterion to acceptable sizes. The crystal contains one DME molecule which could be modeled with acceptable thermal parameters, in addition to other disordered solvent. The solvent was constrained to be a hexane molecule (present as a crystallization solvent), and restraints were employed to treat the displacement parameters. We note the CheckCIF routine produced one Alert A item related to a solvent accessible void of 339 $Å^3$ (4% of the total volume). We were unable to discern any solvent or electron density in this void, likely due to severe disorder. However, this void corresponds to only 103 electrons per cell, which is too few to be a third counterion; thus, this issue should not affect any conclusions drawn about the oxidation state of the complex. The CIF file and CheckCIF file output contain validation reply form items which address this issue.

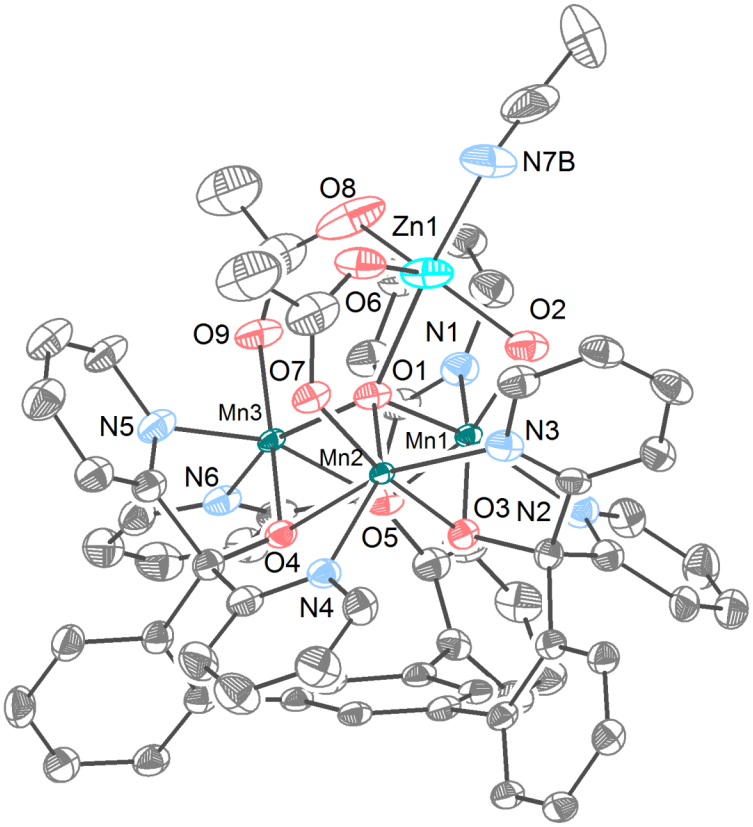

Figure S30. Structural drawing of [**1**-Zn(CH_3CN)]$(OTf)_3$ with 50% probability ellipsoids. Outer-sphere trifluoromethanesulfonate ions and hydrogen atoms not shown for clarity.

Special refinement details for [1-Zn(CH_3CN)]$(OTf)_3$

The structure contains a disordered trifluoromethanesulfonate counterion, which was modeled in two positions. Restraints were employed to treat the angles, distances, and displacement parameters of the counterion. The acetonitrile bound to the zinc center is also disordered, and was refined in two positions using restraints to treat the displacement parameters. The crystal also contains a free molecule of acetonitrile whose population refined to 0.70.

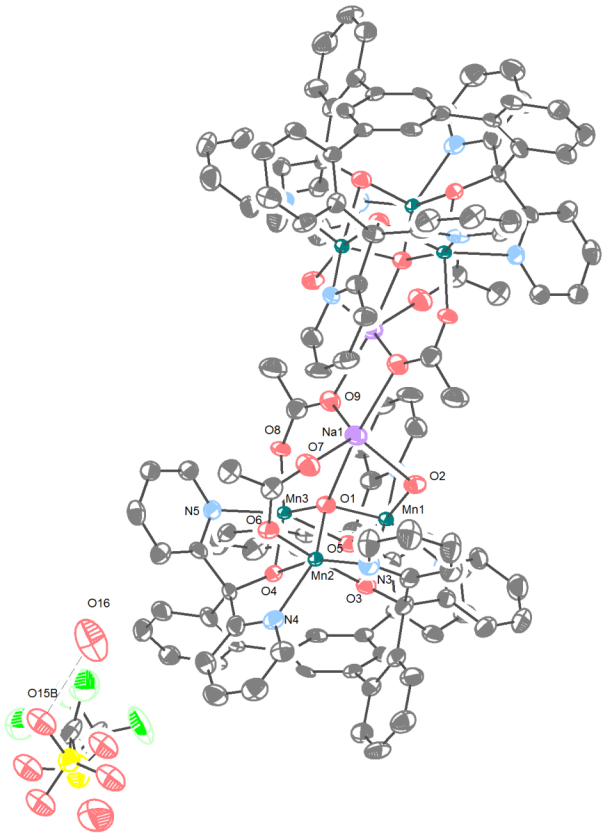

Figure S31. Structural drawing of [**1**-Na]$_2$(OTf)$_4$ with 50% probability ellipsoids. Only one of two triflate counterions is shown to demonstrate H-bonding to the water molecule. Hydrogen atoms not shown for clarity.

Special refinement details for [1-Na]$_2$(OTf)$_4$

The structure contains a disordered trifluoromethanesulfonate counterion, which was modeled in two positions using populations. Restraints were used to treat the bond distances, angles, and displacement parameters of the counterion. Crystals of this compound were weakly diffracting and very little high angle data could be observed. The present data collection and solution represent the best of repeated data collections using a number of different crystals. The CIF file and CheckCIF file output contain validation reply form items which address this issue. Additionally, there was a single area of residual electron density that was modeled as a water molecule at 85% population. This water molecule (O16) is within 2.8 Å of O15B, likely indicating hydrogen bonding. Although these crystals were grown in a dry glovebox, it is possible that trace amounts of moisture entered the mixture over time.

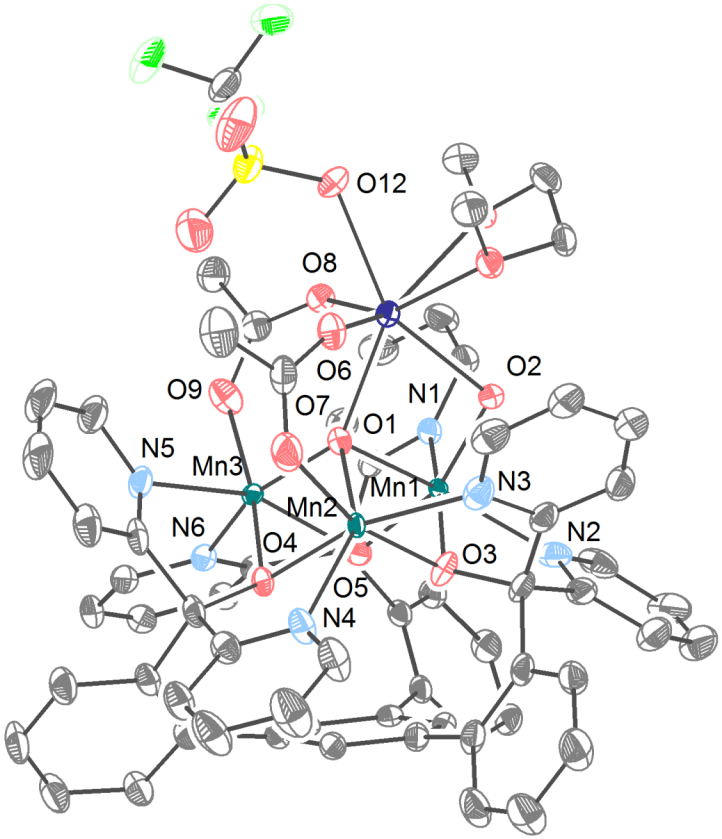

Figure S32. Structural drawing of [**2**-Y(DME)(OTf)](OTf)$_2$ with 50% probability ellipsoids. Outer-sphere trifluoromethanesulfonate ions and hydrogen atoms not shown for clarity.

Special refinement details for [2-Y(DME)(OTf)](OTf)$_2$

The structure contains a molecule of diethyl ether as solvent. The crystal also contains other disordered solvent molecules, presumably diethyl ether and/or 1,2-dimethoxyethane (both present in the crystallization) that could not be satisfactorily modeled. Due to the considerable percentage of the unit cell occupied by the solvent (1496 Å^3, 17%), SQUEEZE was employed to produce a bulk solvent correction to the observed intensities. The program accounted for 448 electrons. This is in reasonable agreement with what would be expected for two disordered molecules of 1,2-dimethoxyethane (400 electrons).

References

1. Saltzman, H.; Sharefkin, J. G., *Organic Synthesis Collective Volumes* **1973,** *5*, 658.
2. Forsberg, J. H.; Spaziano, V. T.; Balasubramanian, T. M.; Liu, G. K.; Kinsley, S. A.; Duckworth, C. A.; Poteruca, J. J.; Brown, P. S.; Miller, J. L. *J. Org. Chem.* **1987**, *52*, 1017.
3. Adhikari, D.; Mossin, S.; Basuli, F.; Huffman, J. C.; Szilagyi, R. K.; Meyer, K.; Mindiola, D. J. *J. Am. Chem. Soc.* **2008**, *130*, 3676.
4. Tsui, E. Y.; Kanaday, J. S.; Day, M. W.; Agapie, T. *Chem. Commun.* **2011**, *47*, 4189.
5. Kanady, J. S.; Tsui, E. Y.; Day, M. W.; Agapie, T. *Science* **2011**, *333* 733.
6. Kambe, K. *J. Phys. Soc. Jpn.* **1950**, *5*, 48.
7. *Matlab*, version 7.10.0.499 (R2010a); The MathWorks, Inc.: Natick, MA 2010.

8. Lee, Y.-M.; Kotani, H.; Suenobu, T.; Nam, W.; Fukuzumi, S. *J. Am. Chem. Soc.* **2008**, *130*, 434.
9. Schardt, B. C.; Hill, C. L. *Inorg. Chem.* **1983**, *22*, 1563.
10. APEX2, Version 2 User Manual, M86-E01078, Bruker Analytical X-ray Systems, Madison, WI, June 2006.
11. Sheldrick, G.M. "SADABS (version 2008/1): Program for Absorption Correction for Data from Area Detector Frames", University of Göttingen, 2008.
12. Sheldrick, G.M. (2008). Acta Cryst. A64, 112-122.
13. Spek, A. L. (2006) PLATON – A Multipurpose Crystallographic Tool, Utrecht University, Utrecht, The Netherlands. Spek, A. L. (1990) Acta Cryst. A46, C34.